2010

Microbial and Mineralogical Characterizations of Soils Collected from the Deep Biosphere of the Former Homestake Gold Mine, South Dakota

Gurdeep Rastogi
South Dakota School of Mines and Technology

Shariff Osman
Lawrence Berkeley National Laboratory

Ravi K. Kukkadapu
Pacific Northwest National Laboratory, ravi.kukkadapu@pnl.gov

Mark Engelhard
Pacific Northwest National Laboratory

Parag A. Vaishampayan
California Institute of Technology

See next page for additional authors

Microb Ecol (2010) 60:539–550
DOI 10.1007/s00248-010-9657-y

SOIL MICROBIOLOGY

Microbial and Mineralogical Characterizations of Soils Collected from the Deep Biosphere of the Former Homestake Gold Mine, South Dakota

Gurdeep Rastogi · Shariff Osman · Ravi Kukkadapu · Mark Engelhard · Parag A. Vaishampayan · Gary L. Andersen · Rajesh K. Sani

Received: 3 January 2010 / Accepted: 13 March 2010 / Published online: 13 April 2010

Abstract A microbial census on deep biosphere (1.34 km depth) microbial communities was performed in two soil samples collected from the Ross and number 6 Winze sites of the former Homestake gold mine, Lead, South Dakota using high-density 16S microarrays (PhyloChip). Soil mineralogical characterization was carried out using X-ray diffraction, X-ray photoelectron, and Mössbauer spectroscopic techniques which demonstrated silicates and iron minerals (phyllosilicates and clays) in both samples. Microarray data revealed extensive bacterial diversity in soils and detected the largest number of taxa in *Proteobacteria* phylum followed by *Firmicutes* and *Actinobacteria*. The archael communities in the deep gold mine environments were less diverse and belonged to phyla *Euryarchaeota* and *Crenarchaeota*. Both the samples showed remarkable similarities in microbial communities (1,360 common OTUs) despite distinct geochemical characteristics. Fifty-seven phylotypes could not be classified even at phylum level representing a hitherto unidentified diversity in deep biosphere. PhyloChip data also suggested considerable metabolic diversity by capturing several physiological groups such as sulfur-oxidizer, ammonia-oxidizers, iron-oxidizers, methane-oxidizers, and sulfate-reducers in both samples. High-density microarrays revealed the greatest prokaryotic diversity ever reported from deep subsurface habitat of gold mines.

Electronic supplementary material The online version of this article (doi:10.1007/s00248-010-9657-y) contains supplementary material, which is available to authorized users.

G. Rastogi · R. K. Sani (✉)
Department of Chemical and Biological Engineering,
South Dakota School of Mines and Technology,
Rapid City, SD 57701, USA
e-mail: Rajesh.Sani@sdsmt.edu

S. Osman · G. L. Andersen
Ecology Department, Earth Sciences Division,
Lawrence Berkeley National Laboratory,
Berkeley, CA 94720, USA

R. Kukkadapu · M. Engelhard
WR Wiley Environmental Molecular Sciences Laboratory,
Pacific Northwest National Laboratory,
Richland, WA 99352, USA

P. A. Vaishampayan
California Institute of Technology, Jet Propulsion Laboratory,
Pasadena, CA 91109, USA

Present Address:
G. Rastogi
Department of Plant Pathology, University of California,
Davis 95616, USA

Introduction

Ultra-deep mines provides a unique access to examine the microbial communities in deep terrestrial subsurface environments where hostile life conditions such as extreme temperature, pH, pressure, low oxygen concentration, no light and toxic metals persist. Several investigations, both culture-based and culture-independent, on gold mines in Japan [13, 14, 23], South Africa [3, 7, 12, 16, 21, 25, 38], Canada [24], and the USA [27, 30] have demonstrated active diverse microbial populations with bewildering metabolic capabilities. These studies also shed light on the spectacular biogeochemistry that governs microbial community composition in deep biosphere where contemporary photosynthetically derived carbon may be absent.

Most of the studies discussed above used 16S rRNA cloning-and-sequencing methods to examine the microbial

community composition in deep gold mine biosphere. Culture-independent methods, in particular polymerase chain reaction (PCR) and the sequencing of clone libraries are considered the "gold standard" for studying microbial diversity [9]. However, a clone library approach is tedious, time-consuming, and limited by the number of clones sequenced primarily because of the high sequencing cost. Thus, a clone library approach is impractical for generating comprehensive microbial molecular inventory in a given sample. While 16S rRNA clone libraries permit an initial survey of diversity, studies have shown that clone libraries with <400 sequences represent only an incomplete sampling of microbial populations and extremely low-abundance organisms remain un-represented [15]. Thus, most published reports on ultra-deep gold mines utilizing cloning-and-sequencing reveal only a small portion of the microbial diversity present in a given sample.

Recently with unprecedented progress in microbial ecology, hybridizing PCR products directly (without cloning) to a 16S rRNA gene microarray (PhyloChip) has emerged as a rapid, reproducible, and more comprehensive way to analyze microbial diversity in soil, water, and air samples [4, 9, 28]. One of the greatest advantages of using high-density microarrays is their capability to detect individual taxa from an environment that may contain as many as 10,000 different microbial types [40]. In addition, by using sequence-specific PCR, studies have validated that low abundant lineages captured by PhyloChips were indeed present in the original environment, despite their absence in corresponding clone libraries [9]. This highlighted the potential superiority of PhyloChips compared to classical clone libraries. Literature suggests that to date such comprehensive microbial census methods were not applied to explore the microbial diversity in mining-impacted deep biosphere of gold mines and hence these microbial communities remain largely uncharacterized.

The Homestake gold mine (44°35′2074″N, 103°75′082″W; Lead, SD) is the deepest mine (2.4 km deep) in the North America and had largest gold deposit ever found in the Western Hemisphere. A full description of the mine can be located at Lawrence Berkeley National Laboratory, CA, website http://www.lbl.gov/nsd/homestake/Reference.html). The mine was closed in December 2001 after more than 125 years of mining. On 10th July 2007, the National Science Foundation (USA) announced this mine as a site for the Deep Underground Science and Engineering Laboratory (DUSEL). This former gold mine offers a unique opportunity for direct deep subsurface exploration. In recent studies, we have cultured the cellulose-degrading bacteria [27] and evaluated the microbial diversity in soil samples collected from the Homestake mine using typical 16S clone libraries [30]. Our results showed that majority (>95%) of the sequences retrieved in clone libraries were most closely related to environmental sequences from yet-uncultured bacteria representing a hitherto unidentified microbial diversity. In addition, rarefaction analysis of clone library generated non-asymptotic plots which indicated that diversity was not exhaustively sampled due to insufficient clone sequencing, a common problem when assessing environmental microbial diversity by using cloning approaches. Thus, a more sensitive method such as microarrays were required for a comprehensive microbial community composition investigation in deep subsurface habitat of the Homestake mine. Therefore, the purpose of the research was to elucidate the microbial community composition in the soil samples collected from the Homestake mine by applying high-density 16S PhyloChips. Furthermore, for the first time, the detailed mineralogical characteristics of soil samples were analyzed using high-resolution techniques such as X-ray diffraction, X-ray photoelectron, and Mössbauer spectroscopy. The phylogenetic features of microbial community present in the Homestake mine were compared with corresponding 16S clone libraries constructed earlier from the same samples [30] and with those of communities from other deep subsurface environments including ultra-deep gold mines.

Materials and Methods

Subsurface Soil Sampling

A schematic cross section and locations of sampling sites in the former Homestake gold mine has been shown in Rastogi et al. [30]. In May 2008, two soil samples were collected corresponding to the Ross shaft and No. 6 Winze of the Homestake mine at a depth of 1.34 km. One sample was directly across the landing from the Ross shaft, one of two primary shafts from the surface into the mine, and one was outside the No. 6 Winze hoist room. Both samples were collected along the junction of the drift wall and the floor, where a small accumulation of soil debris had built up through the years of mining. These areas were not disturbed by any type of activities including human trafficking from June 2003 to May 2008. The outer surfaces of the soil debris built up were discarded and only inner surfaces were collected for microbial diversity analyses using sterile spatulas. This was done to minimize the chances of contamination from exogenous microbes. The temperature at the time of sampling was 26°C which was measured using a mercury thermometer. The samples were transported to South Dakota School of Mines and Technology laboratory (1 h drive) in sterile polypropylene bottles on ice and stored at −20°C until analysis. Soil samples were homogenized in sterile pestle and motor inside a laminar flow hood, and then used for geochemical characterization and DNA extraction.

Mineralogical Characterization of Ross and Winze Soil Samples

The structural characterization of Ross and Winze soils was carried out by Powder X-ray diffraction (XRD) technique for crystalline mineral phases, X-ray photoelectron spectroscopy (XPS) for surface chemical composition and oxidation states, and ^{57}Fe-sensitive Mössbauer for Fe-mineralogy. XRD was carried out with a Philips PW3040/00 X'Pert MPD system, using CuK_{α} radiation with a variable divergent slit and a solid-state detector. The Jade+, V5 (Materials Data, Inc., Livermore, CA) software package was used for data analysis. XPS measurements of soil samples were performed using a Physical Electronics Quantum 2000 Scanning ESCA Microprobe. The X-ray beam used was a 100 W, 10-μm diameter beam that was rastered over a 1.3 mm by 0.2 mm rectangle on the sample. Wide scan data was collected using 117.4 eV pass energy. For the $Ag3d_{5/2}$ line, these conditions produced FWHM (full width at half maximum) of better than 1.6 eV. High-energy resolution spectra were collected using 46.95 eV pass energy. For the $Ag3d_{5/2}$ line, these conditions produced FWHM of better than 0.98 eV. The binding energy (BE) scale was calibrated using the $Cu2p_{3/2}$ feature at 932.62±0.05 eV and Au 4f at 83.96±0.05 eV for known standards. The samples experienced variable degrees of charging and low-energy electrons at ~1 eV, 20 μA and low-energy Ar^{+} ions were used to minimize this charging.

Mössbauer spectra were collected at room temperature using a 50-mCi (initial strength) ^{57}Co/Rh source. The velocity transducer MVT-1000 (WissEL) was operated in a constant acceleration mode (23 Hz, ±12 mm/s). An Ar-Kr proportional counter was used to detect the radiation transmitted through the holder. Data were folded to give a flat background and a zero-velocity position corresponding to the center shift of a metal Fe foil at room temperature. Calibration spectra were obtained with a 25-μm-thick Fe (m) foil and Mössbauer data were modeled with Recoil software (University of Ottawa, Canada) [26].

DNA Extraction, PCR, and PhyloChip Hybridization

Total DNA was extracted from 200 mg of soil samples in duplicate using a PowerSoil™ DNA Isolation Kit (MO Bio, Carlsbad, CA) according to the manufacturer's instructions. This DNA isolation kit was used by majority of the previous microbial diversity studies on deep subsurface gold mines [12–14, 21, 23, 24, 30, 38]. Thus, results obtained in our study could be compared with earlier studies with greater confidence. For PhyloChip hybridization, almost full-length bacterial 16S genes were amplified using bacteria-specific (63f/1392r) primers [17]. Archael 16S genes were amplified using an archaea-specific (Arch 21f/Arch 958r) primer set which generated a partial amplification of ~950 bp [29]. Efforts to amplify full-length archael PCR products from Ross and Winze soil samples were unsuccessful despite variation in several parameters (e.g., annealing temperature, alternative primer sets, DNA concentration). Therefore, partial archaeal-16S PCR products were used for microarray hybridization. A control PCR without DNA was set up to check for any contaminants associated with PCR reagents.

Bacterial (~500 ng product) and archaeal (~100 ng product) PCR products amplified from a soil sample were mixed and then concentrated for PhyloChip hybridization. PCR products were prepared for PhyloChip hybridization as described earlier [9]. In brief, PCR products were purified and concentrated to a volume of 40 μl using MinElute columns (Qiagen, Valencia, CA). The PCR products were then spiked with known amounts of amplicons derived from prokaryotic metabolic genes. The mixture was then fragmented to 50–200 bp fragment using DNase I (Invitrogen, Carlsbad, CA) followed by labeling with a GeneChip DNA labeling kit (Affymetrix, Santa Clara, CA) as per manufacturer's protocol. The labeled DNA was hybridized to PhyloChips (Affymetrix GeneChips), washed and stained as per standard Affymetrix protocol. For detailed information on microarray design, fabrication, and analytic procedures (background subtraction, detection and quantification criteria, and array normalization) see DeSantis et al. [9]. Operational taxonomic units (OTUs) were classified in phylum, class, order, family, subfamily, and species at sequence similarity cut-off values of 80%, 85%, 90%, 92%, 94%, and 97%, respectively [9]. An OTU was considered present in the sample when 90% or more of its assigned probe pairs for its corresponding probe set were positive (positive fraction of >0.90) [9].

Results

Mineralogical Characteristics of Ross and Winze Soil Samples

The Powder XRD identified major crystalline phases. Both sample spectra were qualitatively similar to each other (Fig. 1). They were rich in quartz (SiO_2), chlorite-chamosite [$(Fe_5Al)(AlSi_3)O_{10}(OH)_8$], and annite [$KFe_3AlSi_3O_{10}(OH)_2$] minerals; only the major peaks (100% intensity) of each mineral phase are indicated by arrows in the Fig. 1. Other minor peaks were due to other reflections of annite, chamosite, and quartz phases and the difference in the peak intensities merely reflect different phase composition. Chamosite was detected in relatively higher amounts than annite in the Ross sample while its amount was lower than annite in the Winze sample.

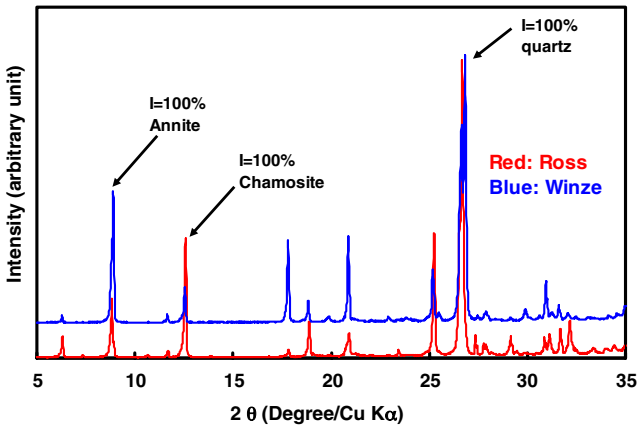

Figure 1 X-ray diffraction patterns of Ross and Winze soils showing major mineral phases of annite, chamosite, and quartz (shown by *arrows*). XRD patterns identified similar features in both samples. Only 100% intense peaks were identified by *arrows*

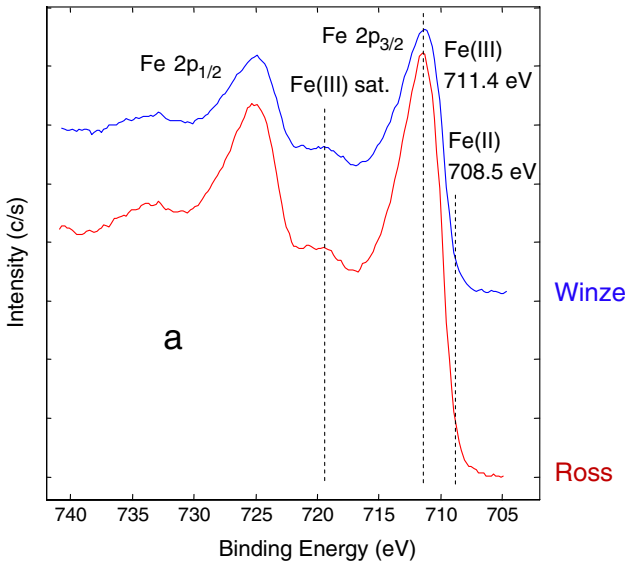

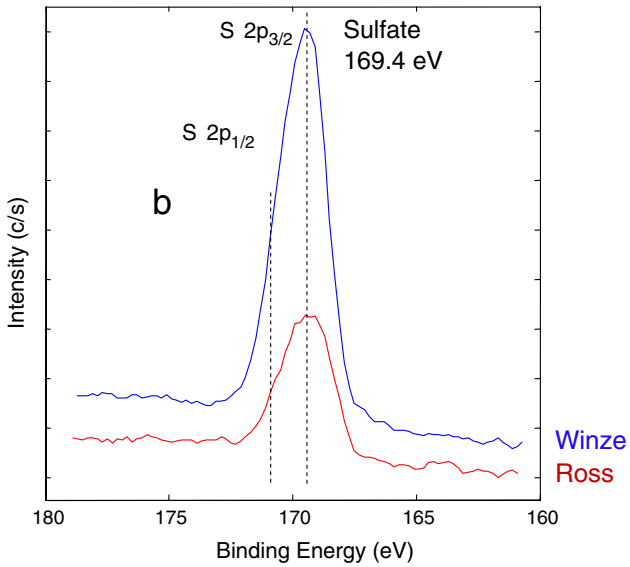

Figure 2 High energy resolution X-ray photoelectron spectra of Ross and Winze soils **a** Fe 2p region and **b** S 2p region showing the presence of Fe(II), Fe(III), and sulfate

XPS can quantify surface chemistry and composition by probing a maximum depth of ~10 nm. High-energy resolution photoemission spectra of the Fe2p region (Fig. 2a) and S2p (Fig. 2b) of both the soil samples were obtained to compare their surface characteristics. The spectra were qualitatively similar to each other, consistent with XRD data. The binding energies of the primary Fe $2p_{3/2}$ at (711.4 eV) were consistent with Fe(III) and the lines at (708.5 eV) indicated a small amount of Fe(II) [6]. The Fe satellite peak position (719.0 eV) and line shape was also consistent with mostly Fe(III). The binding energy for the $S2p_{3/2}$ lines (169.4 eV) was consistent with sulfate. The atomic sulfate concentration in the Winze sample was 3.1 atomic percent as compared with the Ross at 1.3 atomic percent (Fig. 2b).

More detailed insights in the composition of iron minerals were revealed by transmission ^{57}Fe-Mössbauer technique (a 57Fe-specific *bulk* technique; natural abundance of ^{57}Fe is 2.2%). Room temperature Mössbauer spectra of the soil samples were similar to each other, hence, only modeled spectrum of Ross soil was shown in Fig. 3a. The similarity of the spectral features was evident from the comparison (Fig. 3b inset); samples mostly differed from each other in relative composition of phyllosilicate minerals, in agreement with XRD. The Mössbauer spectra were rather complex with a wealth of complimentary information. For example, (a) modeling revealed 20% (Winze) to 45% (Ross) of the total Fe as Fe (II) contributed by chamosite and annite, was significantly different from the surface Fe(II) and Fe(III) composition derived from XPS, (b) presence of Fe(II) and Fe(III) various environments. The various Fe-environments in phyllosilicates was particularly apparent from the modeling. The Fe(II) doublets parameters were similar to Fe(II) in various environments in Fe-rich chlorite mineral (chamosite; [32]), and most probably annite [26]. The outer Fe(II) doublet's Mössbauer parameters (blue trace) were characteristic of *trans*-octahedral Fe(II) in chlorite (or *M2*-site). The inner Fe(II) doublet (red trace), however, appeared to be a mixture of *cis*-octahedaral Fe(II) in chamosite (or *M1* site), and most probably some from annite. This assignment was in good agreement with: (a) annite's Mössbauer parameters, (b) inner-to-outer doublet Fe(II) intensity ratios (~1 in Winze; 0.73 in Ross), which were higher than the pure chamosite (~0.5; [32, 41] and (c) apparent line-shape of the inner Fe(II) doublet in the Winze sample. The inner Fe(II) may also have contributions from Fe present in the interlayer brucite-like sheets of chlorite [36]. Similarly, the assignment of the Fe(III) doublet (black trace) was also

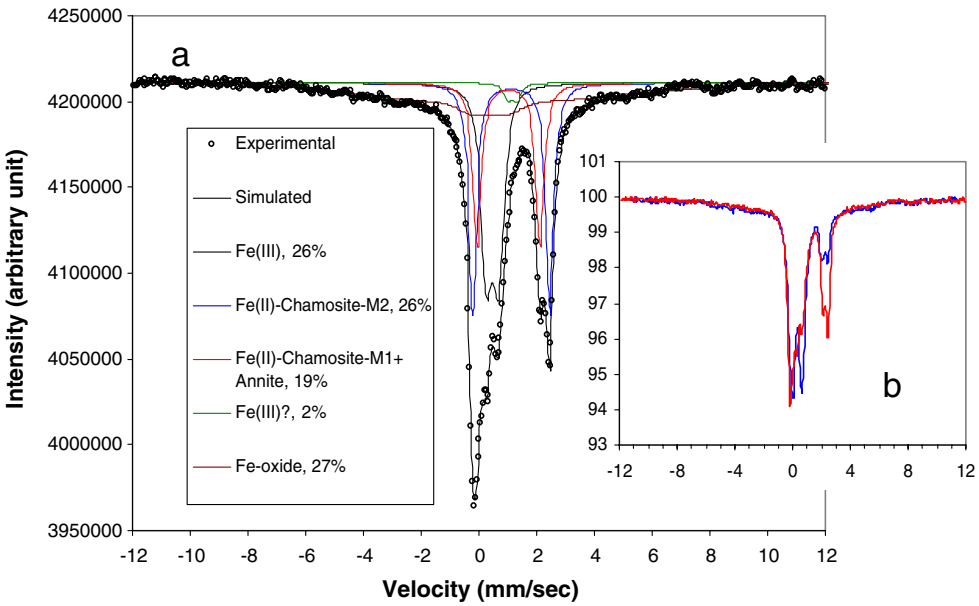

Figure 3 Room temperature Mossbauer spectra: **a** Modeled spectrum of Ross soil showing peaks due to Fe(II) and Fe(III) in chamosite and annite phyllosilicate minerals, and a broad sextet most probably due to small particle or metal-substituted Fe-oxides, and **b** a comparison of both the spectra (unmodeled; *inset*) showing similar Fe-mineralogy

complex, which may have contributions from both octahedral and tetrahedral Fe(III) sites of annite and chamosite, and small-particle (superparamagnetic) Fe-oxide [22]. The broad sextet (brown trace) which was one-third of the total Fe in both the samples was probably due to metal-substituted Fe-oxides (goethite and/or hematite substituted with Al) [22]. These iron oxides were either in amorphous forms or were present in small quantities, since they were not evident in XRD spectra. Absence of sulfide in XPS data also implied the absence of Fe-sulfide minerals in these soil samples.

Deep Biosphere Communities in the Ross Site of the Homestake Mine

PhyloChip proved extremely sensitive in capturing biosignatures at all taxonomic levels and detected a total of 1,511 OTUs positioned within 44 phyla which also included two archaeal phyla namely the *Euryarchaeota* and *Crenarchaeota* (Table 1). These 44 phyla contained diverse taxonomic lineages encompassing 49 classes, 91 orders, and 149 families. Among the 1,511 OTUs captured on the PhyloChip, a total of 25 OTUs were considered unclassified at the phylum level because of their low similarities (<80%) with reference probes on PhyloChip (Table 1). For a comprehensive distribution of bacterial and archaeal OTUs among different classes/orders/families/genera see supplementary tables (Electronic Supplementary Materials, Supplementary Class Table 1; Supplementary Order Table 2; Supplementary Family Table 3, and Supplementary Genera Table 4). PhyloChip data demonstrated that *Proteobacteria* was the most abundant taxa than other phyla, accounting for almost 49% of the total OTUs detected (Table 1). The *Firmicutes* (15% of total OTUs) and *Actinobacteria* (11% of total OTUs) represented the next most abundant phyla on PhyloChip.

Deep Biosphere Communities in the Winze Site of the Homestake Mine

The PhyloChip provided a comprehensive view of microbial diversity and captured a total of 1,678 OTUs spanning 44 phyla, 51 classes, 97 orders, and 154 families in Winze soil sample (Table 1). For a comprehensive distribution of these OTUs among different classes/orders/families/genera see supplementary tables (Electronic Supplementary Materials, Supplementary Class Table 1; Supplementary Order Table 2; Supplementary Family Table 3, and Supplementary Genera Table 4). Of the 1,678 bacterial OTUs detected, a total of 32 OTUs were considered as unclassified at the phylum level (Table 1). Like Ross soil, PhyloChip data for Winze soil indicated that *Proteobacteria* was far more abundant than other phyla, accounting for almost 47% of the total OTUs detected. The *Firmicutes* (15% of total OTUs) and the *Actinobacteria* (12% of total OTUs) represented the next most dominant phyla on the PhyloChip (Table 1).

Discussion

Comparative Species Richness in the Ross and Winze Soils of the Homestake Mine

PhyloChip analysis confirmed the presence of all taxa detected in corresponding 16S clone libraries established earlier from the same samples and additionally demonstrated greater phylotype diversity extending into phyla not observed

Table 1 Bacterial and archael phyla detected in the Ross and Winze sites using PhyloChip analyses

Serial no.	Bacterial/archael phyla detected on PhyloChips	Distribution of OTUs among different phyla	
		Ross site	Winze site
1.	***Acidobacteria***	57	60
2.	***Actinobacteria***	162	198
3.	*AD3*	1	1
4.	***Aquificae***	4	3
5.	***Bacteroidetes***	77	76
6.	*BRC1*	2	1
7.	*Caldithrix*	2	2
8.	*Chlamydiae*	2	2
9.	***Chlorobi***	9	10
10.	***Chloroflexi***	41	38
11.	*Coprothermobacteria*	1	1
12.	***Crenarchaeota***[b]	2	3
13.	*Cyanobacteria*	33	46
14.	***Deinococcus-Thermus***	4	4
15.	*Dictyoglomi*	1	1
16.	*DSS1*	1	1
17.	***Euryarchaeota***[b]	1	3
18.	***Firmicutes***	231	260
19.	***Gemmatimonadetes***	9	9
20.	*LD1PA group*	1	1
21.	*Lentisphaerae*	3	3
22.	*marine group A*	1	2
23.	*Natronoanaerobium*	4	5
24.	*NC10*	1	1
25.	***Nitrospirae***	10	10
26.	*OD1*	1	1
27.	***OP10***	4	5
28.	*OP3*	3	3
29.	*OP8*	2	1
30.	*OP9/JS1*	5	2
31.	***Planctomycetes***	15	11
32.	***Proteobacteria***[c]	732	807
33.	*SPAM*	2	2
34.	***Spirochaetes***	24	35
35.	*Synergistes*	5	5
36.	*Termite group 1*	2	3
37.	*Thermodesulfobacteria*	1	1
38.	*Thermotogae*	1	1
39.	*TM6*	1	1
40.	***TM7***	5	5
41.	Unclassified[a]	25	32
42.	***Verrucomicrobia***	20	19
43.	*WS3*	2	2
44.	*WS5*	1	1

A total of 1,511 and 1,678 OTUs found at the Ross and Winze sites, respectively, were distributed in 44 phyla. Phylum printed in bold are those that have been reported earlier from deep subsurface gold mine environments [13, 23, 24, 28, 38]

[a] A total of 25 and 32 OTUs in the Ross and Winze sites, respectively, could not be assigned to any known phylum and were considered unclassified

[b] Phylum belonging to kingdom *Archaea*

[c] Most abundant phylum in the Ross and Winze sites

by cloning methods [30]. PhyloChip analysis of soil samples obtained from Ross and Winze sites demonstrated 1,511 and 1,678 OTUs, respectively. Comparative PhyloChip data analyses showed that Ross and Winze samples shared large number (1,360) of OTUs in common with only 151 and 318 OTUs exclusively present in Ross and Winze samples, respectively (Fig. 4a). Despite of differences in the physical and chemical composition, both sites had similar microbial communities. Our previous clone library results showed that Ross site had relatively more species richness (110 OTUs) than the Winze site (100 OTUs) as indicated by the number of phylotypes retrieved from the same library sizes (165 clones in each library) [30]. Contrary to earlier clone library data, microarray data showed that Winze site (1678 OTUs) had more species richness than the Ross site (1,511 OTUs). We assume that this was primarily due to the limited number of clones analyzed in our previous study and sequencing of additional clones would have presented more in-depth picture of microbial diversity present in these sites.

A strong linear correlation has been shown earlier between microarray probe set intensity and concentration of OTU-specific 16S rRNA gene copies, which allows relative abundance analysis between normalized PhyloChips [5]. Interestingly, relative abundance based on the fluorescence intensity of OTU probe sets for Ross and Winze samples identified specific bacterial groups which were significantly different between two sites. Bacterial taxa demonstrating significant changes in intensity between Ross and Winze are depicted in Fig. 4b. Though both samples, shared a majority of OTUs, differences in bacterial abundances were observed. We used same DNA extraction protocol for both soil samples therefore assuming the equal extraction efficiencies of various taxa in both soil samples, *Actinobacteria* and bacilli were relatively more abundant in Winze sample as compared to Ross sample. On the other hand bacteria belonging to β-proteobacteria, γ-proteobacteria, δ-proteobacteria, and clostridia were found to be more abundant in Ross sample compared to Winze (Fig. 4b).

Effects of Metals, pH, and Mineral Phases on Microbial Communities

To our surprise, microarray analyses detected a broad phylogenetic diversity in soil samples despite the presence of significant amount of toxic metals and absence of sunlight-irradiation. In our previous study [30], we showed the detailed geochemical characteristics of these soil samples using X-ray fluorescence spectroscopy, coupled plasma optical emission spectrometry, and inductively coupled plasma mass spectroscopy. Our results showed that a significant amounts of toxic metals such as As, Cd, Co, Cr, Cu, Ni, Pb, and Zn were present in Ross and Winze soil samples. However, the water soluble (bioavailable) concentrations of these toxic metals were very low (<0.3 mg/l). Metals are toxic only in their ionic form and pH has been shown a most crucial factor in determining the bioavailability [31]. Roane and Kellogg [31], while studying the bioavailability of Pb in mining-impacted soil samples, showed that soluble toxic Pb concentrations were only detectable in acidic soils. Both the soil samples analyzed in our study had near neutral pH (6.6–6.7) [30] due to which bioavailable metal concentrations will decrease resulting in to less or no toxic effects on the inhabitant deep subsurface microbial communities.

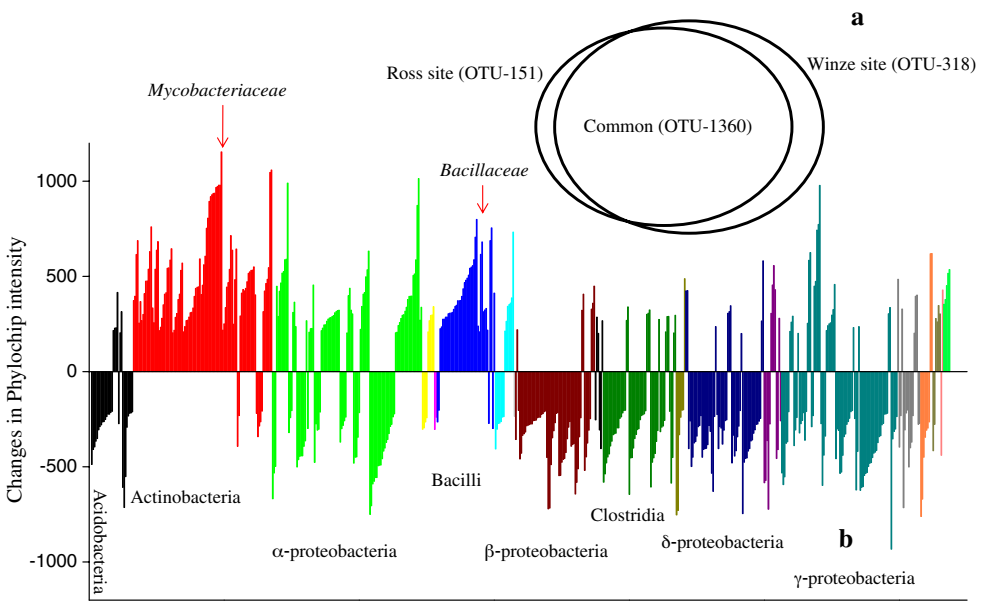

Figure 4 **a** Venn diagram showing fraction of similar OTUs observed between the Ross and Winze samples. The *number in the circle* indicates the estimated numbers of OTUs that are shared between two samples. **b** Comparison of relative abundance of taxa based on fluorescence intensity of OTU probes in Ross and Winze samples. OTUs were arranged based on their taxonomic affiliations. *Bars above the zero line* represent increased abundance in Winze sample relative in Ross sample while *bars below* represent relative decline in abundance in Winze sample

In addition to pH, another important factor controlling metal bioavailability in deep biosphere could be the presence of several complex mineral phases. XRD, XPS, and Mössbauer data indicated the presence of various minerals including chamosite, annite, and unidentified amorphous metal-substituted iron oxides. The surfaces of soil minerals have strong metal ions adsorptive capabilities and therefore may have reduced aqueous concentrations to a non-toxic levels, and decreasing overall metal bioavailability and toxicity [33, 34]. In subsurface soil, ferric oxides and oxyhydroxides (e.g., hematite, goethite, ferrihydrite) commonly exists as soil minerals. These minerals have strong affinity for a large number of cations and anions primarily due to their amorphous nature and high surface area [35]. Pertinent to this, our recent study on Pb toxicity to *Desulfovibrio desulfuricans* G20 also showed that in presence of goethite and quartz, Pb toxicity decreased significantly [34]. However, we acknowledge here that accurate effects of metal stress on microbial diversity can be predicted only when control soil samples from uncontaminated areas are also included in analysis. Such microbial diversity surveys with control samples will also help in identifying those taxa that are uniquely present or more dominant in mining-impacted soils.

Subsurface Microbial Community Composition in the Homestake Mine

To date, earlier studies on ultra-deep gold mines utilized clone libraries and culture-based approach to decipher the microbial community composition and so far no study has reported in-depth characterization of microbial diversity in deep subsurface of gold mines. PhyloChips captured lineages previously reported from ultra-deep gold mines and additionally helped recognize the presence of yet to be identified bacterial lineages at each taxonomic level in both samples. Compared to the microbial diversity assessments from other deep subsurface gold-mines [13, 14, 23, 25, 38], our results showed remarkable similarities at phylum level. The phyla in common were *Euryarchaeota, Crenarchaeota*, *Acidobacteria, Actinobacteria, Bacteroidetes, Chlorobi, Chloroflexi, Firmicutes, Gemmatimonadetes, Nitrospirae, Proteobacteria*, and candidate divisions OP10 and TM7 (Table 1). However, this is the first report for the presence of members of phyla AD3, BRC1, *Cladithrix*, *Coprothermobacteria, Cyanobacteria, Deferribacters, Dictyoglomi*, DSS1, LD1PA group, *Lentisphaerae,* marine group A, NC10, OP3,OP8, OP9, OP10, SPAM, SR1, *Synergists*, *Thermotogae*, termite group 1, TM6, TM7, WS3, and WS5 in ultra-deep gold mines (Table 1). Candidate phyla; OP10 and TM7 sequences were retrieved in 16S clone libraries constructed earlier from Homestake mine soil samples [30].

Earlier studies have shown that *Proteobacteria* constituted a major proportion of the clone libraries established from deep subsurface gold mines samples [13, 25, 30]. The PhyloChip results in this study agreed with earlier reports as *Proteobacteria*-related lineages constituted the most abundant group in both the samples. The ubiquitous nature of the *Proteobacteria* is mostly due to their capabilities to cope with hostile life conditions such as high temperature and pressure, extreme pH, oligotrophic environments, metal-reduction, and metal-resistance which are prerequisite to surviving in mining-impacted deep subsurface environments [1]. *Proteobacterial* genera documented in Ross and Winze sites such as *Acinetobacter*, *Burkholderia,* and *Ralstonia* (Electronic Supplementary Material, Supplementary Genera Table 4) have been reported earlier from metal-contaminated environments and are resistant to metals such as cadmium, copper, nickel, and zinc [1, 29] suggesting that abundance of toxic metals in mining-impacted Ross and Winze soils may have selected these genera. It is interesting to note that within the *Proteobacteria*, PhyloChips have identified genera belonging to *α-Proteobacteria (*e.g., *Sphingomonas, Rhodobacter, Caulobacter, Methylobacterium, Brevundimonas, Bradyrhizobium), β-Proteobacteria (*e.g., *Azoarcus, Acidovorax, Nitrosomonas, Thiobacillus, Comamonas), γ -Proteobacteria; (*e.g., *Pseudomonas, Thiocapsa, Nevskia, Methylococcus, Marinobacter, Stenotrophomonas, Halomonas,* and *δ- Proteobacteria (*e.g., *Desulfovibrio)* that have been described earlier from ultra-deep gold mines of Japan and South Africa [13, 14, 25]. Additionally, bacteria such as *Shewanella surugensis* detected in Ross and Winze sites were previously cultured from deep-sea sediments [20]. These genera indicate an original deep biosphere ecosystem in the Homestake mine. Noticeably, the Homestake mine is geographically distinct from previously studied ultra-deep gold mines or deep subsurface habitats. Thus it was interesting to note such similarities in retrieved phylotypes of the Homestake mine with other deep subsurface environments. In addition to retrieving deep biosphere microbial signatures, PhyloChip also indicated several bacteria (e.g., *Roseobacter*) from the Ross and Winze sites that have not been previously reported from deep subsurface or metal-contaminated environments (Electronic Supplementary Material, Supplementary Genera Table 4). Such genera have been widely shown in pristine environments [15] and probably would have been introduced in Homestake mine deep biosphere during mining operations.

In addition to identifying major taxa such as *Proteobacteria, Firmicutes*, and *Actinobacteria*, PhyloChips also captured other minor phyla such as *Gemmatimonadetes*, *Nitrospirae, Planctomycetes, Spirochaetes,* and *Verrucomicrobia* in both the sites. Although, these phyla have been reported earlier from ultra-deep gold mines [13, 14, 25, 30], their roles in the

ecology of deep biosphere remain unclear. Our study demonstrated very low archaeal diversity (only 3-6 OTUs in *Archaea* domain) in the Homestake mine deep biosphere which agreed well with our previous 16S clone library results which demonstrated only few archael lineages in Ross and Winze samples [30]. It is also likely that low archael diversity observed could be due to partial 16S amplicons used for microarray hybridization. The reference 16S probes attached on PhyloChips were based on sequence information from nearly complete (~1,325 bp) 16S rRNA genes. Therefore, PhyloChip analysis using partial archael 16S PCR products (as generated by Arch 21f/Arch 958r) would have missed hybridization of PCR amplicons with several 16S probes present on the PhyloChip and hence the "present" call for several archael OTUs.

Microarrays also indicated several phylotypes related to phyla for which no cultivated representatives are known. For example in the Ross and Winze sites, phylotype similar to sequences from candidate phyla, e.g., OP3, OP9, OP10, TM6, and TM7 were retrieved. To date no cultivable lineages belonging to these candidate divisions have been isolated in cultures [15]. These bacterial divisions are exclusively represented by environmental sequence data and are unstudied. Other phyla such as *Acidobacteria* and *Verrucomicrobia* contain only few cultured members [15]. Therefore, the physiological roles of any of these bacteria in natural environments including in deep subsurface ecology remain unknown. Our study has avoided over data interpretation based solely on PhyloChip data. Nevertheless, a species molecular inventory is an important initial step in describing unique and dynamic microbial communities, and forms basis for the development of improved culturing methods, and subsequently, elucidation of metabolic roles.

Metabolic Versatility in Deep Biosphere of the Homestake Mine

Deep subsurface environments are generally considered as oligotrophic due to the lack of photosynthetically derived electron donors [16]. Geochemical conditions in the subsurface biosphere such as nutrient availability and permeability, soil composition, redox potential, and a variety of other factors generally influence the resident microbial communities. In such environments the geothermal aquifer is the major source of carbon (e.g., methane, carbon dioxide) and energy (e.g., hydrogen, sulfide, reduced iron, and ammonium), and acts as a determinant for microbial community structures. Chemolithoautotrophic microorganisms in deep subsurface that could grow on hydrogen and carbon dioxide (e.g., acetogenic bacteria) can act as primary producers, initiating heterotrophic food chains independent of photosynthesis [16]. Active chemolithotrophic bacteria in the ultra-deep gold mines of South Africa and Japan have been reported earlier [3, 23, 38]. These studies have also demonstrated sulfate-reducing and methanogenic metabolic pathways in deep biosphere of gold mines. More interestingly, viable sulfate-reducers, methanotrophs, ammonia-oxidizers, nitrite-oxidizers, methane-oxidizers, and sulfur-oxidizers have been isolated from geothermal water sampled from deep Japanese gold mines [13].

Precambrian aquifer water was pumped continuously for dewatering during the operation of the Homestake mine and in June 2003, pumps were turned off. Current water inflow to the underground is about 2,839 L min^{-1} [8]. Geothermal water enters the Homestake mine from the surface primarily through the shaft and airways that intersect with the open pit. Our previous study, reported a variety of soluble ions (such as SO_4^- [9,237–15,156 mg L^{-1}], and NO_3^- [16–39 mg L^{-1}]) in soils collected from the Ross and Winze sites of the Homestake mine [30]. In present study, soil XPS analysis also identified considerable sulfur mainly in form of SO_4^- ions. These soluble ions can fuel the growth of various chemotrophic microorganisms in deep Homestake mine biosphere where the energy sources are limited. For example, PhyloChip has indicated several chemolithotrophic genera such as ammonia-oxidizers (e.g., *Nitrosomonas* sp.), nitrite-oxidizers (e.g., *Nitrospira* sp.), methane-oxidizers (e.g., *Methylosinus* sp.), sulfur-oxidizers (e.g., *Thiobacillus* sp), methanogens (e.g., *Methanosarcina* sp.), and sulfate-reducers (e.g., *Desulfosporoinus* sp.) in Ross and Winze soils samples. Interestingly, our laboratory enrichment studies for sulfate-reducing bacteria using acetate and sulfate as electron donor and acceptor, respectively, confirmed the existence of viable population of sulfate-reducers in Ross and Winze soil samples. A 16S clone library analysis of the enrichment culture revealed that *Desulfosporosinus* spp. were the dominant lineages in the sulfate-reducing enrichment (Rastogi et al., unpublished data).

The gold deposits at the Homestake mine are typically associated with the banded ironstone formation [2] therefore both soil samples contained very high amount of iron; 51,540–75,657 mg L^{-1} [30]. In this study, XPS and Mössbauer data clearly showed the presence of reduced iron [Fe(II)]. As expected, PhyloChip detected several Fe-oxidizing bacteria (e.g., *Leptothrix, Acidithiobacillus*) in both soil samples. These bacteria proliferate in habitats where anaerobic Fe(II)-rich water comes in the contact of air. During dewatering of the Homestake mine for the construction of DUSEL, the exposed oxygenated Fe(II)-rich surfaces served as a primary site for the growth of these bacteria, evident by the characteristic rust colored soil samples from insoluble Fe(III)-ions [30]. Room temperature Mossbauer spectra showed >25% of the iron in form of

oxidized Fe(III)-ions. In addition to Fe-oxidizing bacteria, microarrays also captured few Fe(III)-reducing bacteria such as *Shewanella* sp. in both site that can reduce variety of terminal electron acceptors, including nitrate, nitrite, thiosulfate, and elemental sulfur [11]. In a 16S clone library of Fe-reducing enrichment cultures initiated using Ross and Winze soils with acetate and hematite as electron donor and acceptor, respectively showed that *Clostridium* sp. dominated the iron-reducing communities (Rastogi et al. unpublished data). PhyloChips also indicated *Clostridium*-related OTUs in both soil samples (Electronic Supplementary Material, Supplementary Genera Table 4).

Another important chemotrophic group of bacteria in the Homestake mine could be sulfur-oxidizers because of the significant amount of sulfur (as shown by XPS) present in soil samples. Chemical characterization of Ross and Winze soil also showed significant sulfur (1.79–2.66%; measured as total sulfur) which can act as energy source for these bacteria [30]. As a proof to this hypothesis, we have cultured sulfur-oxidizing bacteria belonging to genus *Thiobacillus* from Ross and Winze soil samples (Rastogi et al., unpublished data). PhyloChip data also demonstrated the presence of *Thiobacillus* sp. in soil samples. Interestingly, *Thiobacilli* are chemolithoautotrophic, sulfur-oxidizing bacteria that are restricted to habitats where both an electron donor (reduced sulfur compounds [S^0, H_2S, and $S_2O_3^{-2}$] or Fe (II) in some cases) and an electron acceptor (O_2 or NO_x) simultaneously exist. These bacteria produce sulfuric acid and Fe(III) as by-products of their metabolism and play a very important role in biomineralization. Southam et al. [37] further demonstrated a very strong physical association between *Thiobacillus* species and the sulfide minerals, which helps account for their prominence in tailings environments.

Alternative carbon sources such as lignocelluloses may also fuel the Homestake mine deep biosphere. During active mining-operations for over 125 years, lignocellulosic substrates were introduced into the Homestake mine [27]. Interestingly, we have isolated several strains of *Bacillus, Paenibacillus*, and *Geobacillus* from the Homestake mine that were able to grow on cellulose and sawdust (a fine powder of woodchips) as a source of carbon and energy [27]. All these genera have been captured by PhyloChips which indicates that Homestake mine deep biosphere harbors microbial communities that can use complex lignocellulosic materials as carbon and energy sources.

Molecular-based diversity methods (e.g., PCR, cloning-and-sequencing, PhyloChip) based on direct DNA/RNA-extraction are alternative to classical culture-based methods, and have provided great insights in to community composition, richness, and structure of microbial communities. However, like culture-based methods, these molecular methods have their own pitfalls and are associated with bias at every step. Bias associated with DNA extraction (e.g., incomplete/no lyses of microbial cells) can distort the revealed community composition, richness, and microbial community structure [10]. In addition, all PCR-based diversity studies have additional biases associated which include primer choice, annealing temperature, and preferential amplification of certain templates [39].

DNA extraction from environmental samples constitutes the first step in PCR-based community analysis. In fact, different DNA recovery methods have been shown to reveal different depth of microbial diversity due to variation in the ability to break open cells/spores [18]. Different studies have used different DNA extraction protocols in soil microbial diversity analysis. The primary reason so many methods for DNA extraction have been used is due to the fact that most procedures are optimized for a specific soil. This implies that any given procedure may not be universally applicable to all soils due to inherent spatial and microbial heterogeneity [42]. Use of a standard DNA extraction protocol which is efficient for a soil sample may or may not work for other samples sometimes even collected from the same site. DNA extraction efficiency is correlated with soil's physicochemical characteristics (texture, particle size), inhibitors (humic acids, metals, organic legends, etc.), and type of microbial communities.

Feinstein et al. [10] demonstrated that biases in community analysis can be reduced in many situations by pooling three successive DNA yields from a recovery method. Another study by McIlroy et al. [19] suggested use of several validated DNA extraction methods and pooled DNA extracts to minimize any risk of bias. Use of such validated protocols by all microbial ecologists could provide a more complete understanding of the soil microbial community composition and would offer a platform where quantitative inter-comparisons can be made [18]. In addition, development of a single method for purification of DNA from all soil samples will be a great step toward automating the procedures, and for standardizing results between laboratories. A procedure that is equally efficient for all soil samples, efficiently lyses all bacterial groups, requires little time to complete, and is easy to processing multiple samples simultaneously would be highly desirable. For example, MoBio PowerSoil™ DNA isolation kit which is also used in our study is very widely used method for isolating microbial DNA of the highest quality and purity from most environmental samples including deep subsurface gold mines. An advantage of using commercially available kits for DNA isolation is that they provide a rapid and standardized approach that can be quickly learned. Nonetheless, working with complex environmental samples, e.g., soil where >99% microorganisms have not been cultured yet; it is difficult to predict the efficiency of MoBio PowerSoil™ kit for those uncultured organisms. In

addition, it would be worth to acknowledge that although, microarray technology has been used for specific, quantitative, and high-throughput detection of microbial diversity in natural settings; it is unreliable in identifying and detecting novel prokaryotic taxa. The ecological importance of a species, which may be abundant and pivotal to the ecosystem under study, can be completely ignored if the species does not have a corresponding probe on the PhyloChip. Furthermore, community analysis using molecular methods alone is not sufficient for predicting the metabolic functions within the environment.

In summary, the present study provided a comprehensive microbial census on the bacterial and archael communities in the mining-impacted deep subsurface habitat of the Homestake mine. In comparison to previous studies, the use of high-density microarrays resulted in identification of enormous phylogenetic diversity from ultra-deep gold mines. We acknowledge here that molecular oxygen and surface microbes were introduced into the Homestake mine by human activities during mining-operations, thus the microbial community in soil samples does not necessarily reflect an indigenous deep subsurface microbial population. However, various environmental limitations in the deep biosphere of the Homestake mine would shape the microbial diversity as a novel and unique subsurface microbial ecosystem. The results on microbial diversity and geochemistry will serve as a vital comparison for future assessment of changes in microbial diversity and geochemistry as re-entry in Homestake mine continues and the deeper levels become exposed during the construction of the DUSEL.

Acknowledgements This research was funded by the South Dakota Board of Regents Competitive Research Grant (Award No. SDBOR/SDSMT 2010-09-05). Powder XRD, XPS, and Mössbauer spectroscopy measurements were conducted using EMSL, a national scientific user facility sponsored by the Department of Energy's Office of Biological and Environmental Research located at Pacific Northwest National Laboratory. We would like to acknowledge Colleen Russell (PNNL) for her help in XRD measurements and Mössbauer sample preparations. Authors appreciate the assistance provided by Dr. L. D. Stetler of Department of Geology and Geological Engineering, SDSM&T in sample collection. We also would like to thank the anonymous reviewers whose critiques were instrumental in improving the quality of manuscript.

References

1. Akob DM, Mills HJ, Kostka JE (2007) Metabolically active microbial communities in uranium-contaminated subsurface sediments. FEMS Microbiol Ecol 59:95–107
2. Bachman RL, Caddey SW (1990) The Homestake mine, lead, South Dakota: an overview. In: Paterson CJ, Lisenbee AL (eds) Metallogeny of gold in the Black Hills, South Dakota. Society of Economic Geologists Guidebook Series, v. 7, pp. 129–135
3. Baker BJ, Moser DP, MacGregor BJ, Fishbain S, Wagner M, Fry NK, Jackson B, Speolstra N, Loos S, Takai K, Lollar BS, Fredrickson J, Balkwill D, Onstott TC, Wimpee CF, Stahl DA (2003) Related assemblages of sulphate-reducing bacteria associated with ultradeep gold mines of South Africa and deep basalt aquifers of Washington State. Environ Microbiol 5:267–277
4. Brodie EL, Desantis TZ, Joyner DC, Baek SM, Larsen JT, Andersen GL, Hazen TC, Richardson PM, Herman DJ, Tokunaga TK, Wan JM, Firestone MK (2006) Application of a high-density oligonucleotide microarray approach to study bacterial population dynamics during uranium reduction and reoxidation. Appl Environ Microbiol 72:6288–6298
5. Brodie EL, DeSantis TZ, Parker JP, Zubietta IX, Piceno YM, Andersen GL (2007) Urban aerosols harbor diverse and dynamic bacterial populations. Proc Natl Acad Sci USA 104:299–304
6. Chambers SA, Kim YJ, Gao Y (2008) Fe2p core-level spectra for pure, epitaxial α-Fe_2O_3(0001), γ-Fe_2O_3(001), and Fe_3O_4(001). Surf Sci Spectra 5:219–228
7. Chivian D, Brodie EL, Alm EJ, Culley DE, Dehal PS, DeSantis TZ, Gihring TM, Lapidus A, Lin LH, Lowry SR, Moser DP, Richardson PM, Southam G, Wanger G, Pratt LM, Andersen GL, Hazen TC, Brockman FJ, Arkin AP, Onstott TC (2008) Environmental genomics reveals a single-species ecosystem deep within Earth. Science 10:275–278
8. Davis A, Roggenthen W, Stetler L, Hladysz Z, Johnson C (2009) Post-closure flooding of the Homestake mine at Lead, South Dakota. Mining Engineering, March. pp. 43–47
9. DeSantis TZ, Brodie EL, Moberg JP, Zubieta IX, Piceno YM, Andersen GL (2007) High-density universal 16S rRNA microarray analysis reveals broader diversity than typical clone library when sampling the environment. Microb Ecol 53:371–383
10. Feinstein LM, Sul WJ, Blackwood CB (2009) Assessment of bias associated with incomplete extraction of microbial DNA from soil. Appl Environ Microbiol 75:5428–5433
11. Fredrickson JK, Romine MF, Beliaev AS, Auchtung JM, Driscoll ME, Gardner TS, Nealson KH, Osterman AL, Pinchuk G, Reed JL, Rodionov DA, Rodrigues JL, Saffarini DA, Serres MH, Spormann AM, Zhulin IB, Tiedje JM (2008) Towards environmental systems biology of *Shewanella*. Nat Rev Microbiol 6:592–603
12. Gihring TM, Moser DP, Lin L-H, Davidson M, Onstott TC, Morgan L, Milleson M, Kieft TL, Trimarco E, Balkwill DL, Dollhopf ME (2006) The distribution of microbial taxa in the subsurface water of the Kalahari Shield, South Africa. Geomicrobiol J 23:415–430
13. Hirayama H, Takai K, Inagaki F, Yamato Y, Suzuki M, Nealson KH, Horikoshi K (2005) Bacterial community shift along a subsurface geothermal water stream in a Japanese gold mine. Extremophiles 9:169–184
14. Inagaki F, Takai K, Hirayama H, Yamato Y, Nealson KH, Horikoshi K (2003) Distribution and phylogenetic diversity of the subsurface microbial community in a Japanese epithermal gold mine. Extremophiles 7:307–317
15. Janssen PH (2006) Identifying the dominant soil bacterial taxa in libraries of 16S rRNA and 16S rRNA genes. Appl Environ Microbiol 72:1719–1728
16. Lin LH, Wang PL, Rumble D, Lippmann-Pipke J, Boice E, Pratt LM, Sherwood Lollar B, Brodie EL, Hazen TC, Andersen GL, DeSantis TZ, Moser DP, Kershaw D, Onstott TC (2006) Long-term sustainability of a high-energy, low-diversity crustal biome. Science 20:479–482
17. Marchesi JR, Sato T, Weightman AJ, Martin TA, Fry JC, Hiom SJ, Dymock D, Wade WG (1998) Design and evaluation of useful bacterium-specific PCR primers that amplify genes coding for bacterial 16S rRNA. Appl Environ Microbiol 64:795–799
18. Martin-Laurent F, Philippot L, Hallet S, Chaussod R, Germon JC, Soulas G, Catroux G (2001) DNA extraction from soils: old bias

for new microbial diversity analysis methods. Appl Environ Microbiol 67:2354–2359
19. McIlroy SJ, Porter K, Seviour RJ, Tillett D (2009) Extracting nucleic acids from activated sludge which reflect community population diversity. Antonie Van Leeuwenhoek 96:593–605
20. Miyazaki M, Nogi Y, Usami R, Horikoshi K (2006) *Shewanella surugensis* sp. nov., *Shewanella kaireitica* sp. nov. and *Shewanella abyssi* sp. nov., isolated from deep-sea sediments of Suruga Bay, Japan. Int J Syst Evol Microbiol 56:1607–1613
21. Moser DP, Onstott TC, Fredrickson JK, Brockman FJ, Balkwill DL, Drake GR, Pfiffner SM, White DC, Takai K, Pratt LM, Fong J, Sherwood Lollar B, Slater G, Phelps TJ, Spoelstra N, Deflaun M, Southam G, Welty AT, Baker BJ, Hoek J (2003) Temporal shifts in the geochemistry and microbial community structure of an ultradeep mine borehole following isolation. Geomicrobiol J 20:517–548
22. Murad E, Cashion J (2004) Mossbauer spectroscopy of environmental materials and their industrial utilization, chapter 5. Kluwer Academic Publishers, Norwell
23. Nunoura T, Hirayama H, Takami H, Oida H, Nishi S, Shimamura S, Suzuki Y, Inagaki F, Takai K, Nealson KH, Horikoshi K (2005) Genetic and functional properties of uncultivated thermophilic crenarchaeotes from a subsurface gold mine as revealed by analysis of genome fragments. Environ Microbiol 7:1967–1984
24. Onstott TC, McGown DJ, Bakermans C, Ruskeeniemi T, Ahonen L, Telling J, Soffientino B, Pfiffner SM, Sherwood-Lollar B, Frape S, Stotler R, Johnson EJ, Vishnivetskaya TA, Rothmel R, Pratt LM (2009) Microbial communities in subpermafrost saline fracture water at the lupin Au mine, nunavut, Canada. Microb Ecol 58:786–807
25. Onstott TC, Moser DP, Pfiffner SM, Fredrickson JK, Brockman FJ, Phelps TJ, White DC, Peacock A, Balkwill D, Hoover R, Krumholz LR, Borscik M, Kieft TL, Wilson R (2003) Indigenous and contaminant microbes in ultradeep mines. Environ Microbiol 5:1168–1191
26. Rancourt Ping (1991) Voigt-based methods for arbitrary-shape static hyperfine parameter distributions in Mossbauer spectroscopy. Nucl Instrum Methods Phys Res B 58:85–97
27. Rastogi G, Muppidi GL, Gurram RN, Adhikari A, Bischoff KM, Hughes SR, Apel WA, Bang SS, Dixon DJ, Sani RK (2009) Isolation and characterization of cellulose-degrading bacteria from the deep subsurface of the Homestake gold mine, Lead, South Dakota, USA. J Ind Microbiol Biotechnol 36:585–598
28. Rastogi G, Osman S, Vaishampayan PA, Andersen GL, Stetler LD, Sani RK (2009) Microbial diversity in uranium mining-impacted soils as revealed by high-density 16S microarray and clone library. Microb Ecol 59:94–108
29. Rastogi G, Sani RK, Peyton BM, Moberly JG, Ginn TR (2009) Molecular studies on the microbial diversity associated with mining-impacted Coeur d' Alene river sediments. Microb Ecol 58:129–139
30. Rastogi G, Stetler LD, Peyton BM, Sani RK (2009) Molecular analysis of prokaryotic diversity in the deep subsurface of the former Homestake gold mine, South Dakota, USA. J Microbiol 47:371–384
31. Roane TM, Kellogg ST (1996) Characterization of bacterial communities in heavy metal contaminated soils. Can J Microbiol 42:593–603
32. Rozenson I, Bauminger EA, Heller-Kallai L (1979) Mossbauer spectra of iron in 1:1 phyllosilicates. Am Mineral 64:893–901
33. Sani RK, Peyton BM, Amonette JE, Geesey GG (2004) Reduction of uranium(VI) under sulfate reducing conditions in the presence of Fe(III)-(hydr)oxides. Geochim Cosmochim Acta 68: 2639–2648
34. Sani RK, Rastogi G, Moberly JG, Dohnalkova A, Ginn TR, Spycher N, Shende N, Peyton BM (2010) The toxicity of lead to *Desulfovibrio desulfuricans* G20 in the presence of goethite and quartz. J Basic Microbiol 50:160–170
35. Schwertmann U, Cornell RM (1991) Iron oxides in the laboratory, preparation and characterization. VSH Publishers, New York
36. Smyth JR, Dyar MD, May HM, Bricker OP, Acker JG (1997) Crystal structure refinement and Mossbauer spectroscopy of ordered, triclinic clinochlore. Clays Clay Minerals 45:544–550
37. Southham G, Beveridge TJ (1992) Enumeration of thiobacilli within pH-neutral and acidic mine tailings and their role in the development of secondary mineral soil. Appl Environ Microbiol 58:1904–1912
38. Takai K, Moser DP, DeFlaun M, Onstott TC, Fredrickson JK (2001) Archaeal diversity in waters from deep South African gold mines. Appl Environ Microbiol 67:5750–5760
39. von Wintzingerode F, Göbel UB, Stackebrandt E (1997) Determination of microbial diversity in environmental samples: pitfalls of PCR-based rRNA analysis. FEMS Microbiol Rev 21: 213–229
40. Wilson KH, Wilson WJ, Radosevich JL, DeSantis TZ, Viswanathan VS, Kuczmarski TA, Andersen GL (2002) High-density microarray of small-subunit ribosomal DNA probes. Appl Environ Microbiol 68:2535–2541
41. Yershova ZO, Nikitina AP, Perfileve Yu.D, Baeshkin AM (1975) Study of chamosites by gamma-resonance (Mossbauer) spectroscopy. Proc. International Clay Conference, Mexico. pp. 211–220
42. Zhou J, Bruns MA, Tiedje JM (1996) DNA recovery from soils of diverse composition. Appl Environ Microbiol 62:316–322

Supplementary class Table 1: Bacterial and archael classes detected in the Ross and Winze sites using PhyloChip analyses

Serial No.	Bacterial/archael classes detected on PhyloChips	Distribution of OTUs among different classes	
		Ross site	**Winze site**
1.	*Acidobacteria*	34	35
2.	*Acidobacteria-10*	1	1
3.	*Acidobacteria-4*	3	3
4.	*Acidobacteria-5*	1	1
5.	*Acidobacteria-6*	13	17
6.	*Actinobacteria*	160	196
7.	*Alphaproteobacteria*†	263	279
8.	*Anaerolineae*	21	19
9.	*Aquificae*	4	3
10.	*Bacilli*	86	96
11.	*Bacteroidetes*	21	29
12.	*BD2-10 group*	2	2
13.	*Betaproteobacteria*	125	134
14.	*C1*×	2	2
15.	*Catabacter*	6	6
16.	*CH21 cluster*	2	3
17.	*Chlamydiae*	2	2
18.	*Chlorobia*	3	3
19.	*Chloroflexi-3*	2	2
20.	*Chloroflexi-4*	2	2
21.	*Clostridia*	123	135
22.	*Cyanobacteria*	23	34
23.	*Dehalococcoidetes*	9	8
24.	*Deltaproteobacteria*	91	97
25.	*Desulfotomaculum*	4	6
26.	*Dictyoglomi*	1	1
27.	*Epsilonproteobacteria*	28	34
28.	*Flavobacteria*	29	21
29.	*Gammaproteobacteria*	218	255
30.	*gut clone group*	2	2
31.	*JS1*	3	ND
32.	*KSA1*	1	1
33.	*Methanomicrobia*×	ND	1
34.	*mgA-1*	ND	1
35.	*mgA-2*	1	1
36.	*Mollicutes*	7	10
37.	*Nitrospira*	10	10

38.	*OP11-5*	1	1
39.	*OP9*	2	2
40.	*Planctomycetacia*	15	11
41.	*Solibacteres*	3	2
42.	*Sphingobacteria*	24	24
43.	*Spirochaetes*	24	35
44.	*Symbiobacteria*	2	2
45.	*Thermodesulfobacteria*	1	1
46.	*Thermomicrobia*	2	2
47.	*Thermoplasmata*×	1	2
48.	*Thermoprotei*	ND	1
49.	*Thermotogae*	1	1
50.	*TM7-3*	2	2
51.	Unclassified¶	113	124
52.	*Verrucomicrobiae*	17	16

A total of 1511 and 1678 OTUs found at the Ross and Winze sites respectively were distributed in 49 and 51 classes.

† Most abundant class in the Ross and Winze site.

¶ A total of 113 and 124 OTUs in the Ross and Winze sites, respectively could not be assigned to any known class and were considered unclassified.

ND- Not detected

× Class belonging to kingdom *Archaea*

Supplementary order Table 2

Bacterial and archael orders detected in the Ross and Winze sites using PhyloChip analyses

Serial No.	Bacterial/archael orders detected on PhyloChips	Distribution of OTUs among different orders	
		Ross site	Winze site
1.	*Acetobacterales*	4	5
2.	*Acholeplasmatales*	1	3
3.	*Acidimicrobiales*	13	14
4.	*Acidithiobacillales*	7	6
5.	*Acidobacteriales*	34	34
6.	*acidophile isolate group*	1	ND
7.	*Actinomycetales*†	132	162
8.	*Aeromonadales*	3	2
9.	*Alteromonadales*	27	32
10.	*AMD clone group*	5	5
11.	*Anaeroplasmatales*	4	4
12.	*aquatic clone group*	3	3
13.	*Aquificales*	4	3
14.	*Azospirillales*	7	7
15.	*Bacillales*	67	68
16.	*Bacteroidales*	21	29
17.	*Bdellovibrionales*	2	2
18.	*Bifidobacteriales*	1	7
19.	*Bradyrhizobiales*	49	58
20.	*Burkholderiales*	74	84
21.	*C1a*×	ND	1
22.	*C1b*×	1	ND
23.	*Caldithrales*	2	2
24.	*Campylobacterales*	28	34
25.	*Caulobacterales*	11	10
26.	*Chlamydiales*	2	2
27.	*Chlorobiales*	3	3
28.	*Chloroflexi-1a*	6	7
29.	*Chloroflexi-1b*	2	2
30.	*Chloroflexi-1f*	2	2
31.	*Chloroplasts*	16	17
32.	*Chromatiales*	19	24
33.	*Chroococcales*	1	1
34.	*Clostridiales*	121	132
35.	*Consistiales*	8	7
36.	*Coriobacteriales*	2	2

37.	*dechlorinating clone group*	1	1
38.	*Desulfobacterales*	25	25
39.	*Desulfovibrionales*	11	13
40.	*Desulfurococcales*×	ND	1
41.	*Desulfuromonadales*	6	5
42.	*Devosia*	ND	1
43.	*Dictyoglomales*	1	1
44.	*EB1021 group*	4	4
45.	*Ellin307/WD2124*	2	2
46.	*Ellin314/wr0007*	5	7
47.	*Ellin329/Riz1046*	3	3
48.	*Ellin6075/11-25*	2	2
49.	*Ellin6095/SC-I-39*	2	2
50.	*Enterobacteriales*	21	46
51.	*Flavobacteriales*	29	21
52.	*GAO cluster*	4	4
53.	*Holophagales*	ND	1
54.	*Hydrogenophilales*	2	2
55.	*Lactobacillales*	19	28
56.	*Legionellales*	12	11
57.	*Methanosarcinales*×	ND	1
58.	*Methylococcales*	7	9
59.	*Methylophilales*	1	1
60.	*MND1 clone group*	4	4
61.	*Mycoplasmatales*	1	2
62.	*Myxococcales*	16	15
63.	*Neisseriales*	6	6
64.	*Nitrosomonadales*	13	15
65.	*Nitrospirales*	10	10
66.	*Nostocales*	1	6
67.	*Oceanospirillales*	8	13
68.	*Oscillatoriales*	1	3
69.	*Pasteurellales*	2	2
70.	*Planctomycetales*	14	11
71.	*Plectonema*	3	3
72.	*Prochlorales*	ND	1
73.	*Pseudanabaena*	ND	1
74.	*Pseudomonadales*	38	37
75.	*Rhizobiales*	60	66
76.	*Rhodobacterales*	55	39
77.	*Rhodocyclales*	16	13
78.	*Rickettsiales*	9	10
79.	*Roseiflexales*	2	2
80.	*Rubrobacterales*	6	5
81.	*SAR86*	1	1

82.	*Scytonema*	ND	1
83.	*Sphingobacteriales*	24	24
84.	*Sphingomonadales*	24	38
85.	*Spirochaetales*	24	35
86.	*Spirulina*	1	1
87.	*SUP05*	3	3
88.	*Symbiobacterales*	2	2
89.	*Symbionts*	4	5
90.	*Syntrophobacterales*	12	14
91.	*Thermodesulfobacteriales*	1	1
92.	*Thermotogales*	1	1
93.	*Thiotrichales*	13	9
94.	Unclassified¶	264	282
95.	*uranium waste clones*	2	2
96.	*Verorhodospirilla*	2	1
97.	*Verrucomicrobiales*	17	16
98.	*Vibrionales*	ND	3
99.	*WPS-1*	1	ND
100.	*Xanthomonadales*	10	10

A total of 1511 and 1678 OTUs found at the Ross and Winze sites respectively were distributed in 91 and 97 orders.

† Most abundant order in the Ross and Winze site.

¶ A total of 264 and 282 OTUs in the Ross and Winze sites, respectively could not be assigned to any known order and were considered unclassified.

× Order belonging to kingdom *Archaea*

ND- Not detected

Supplementary family Table 3

Bacterial and archael families detected in the Ross and Winze sites using PhyloChip analyses

Serial No.	Bacterial/Archael families detected on the PhyloChips	Distribution of OTUs among different families	
		Ross site	Winze site
1.	*Acetobacteraceae*	2	2
2.	*Acholeplasmataceae*	1	3
3.	*Acidimicrobiaceae*	8	9
4.	*Acidithiobacillaceae*	7	6
5.	*Acidobacteriaceae*	34	34
6.	*Acidothermaceae*	1	1
7.	*Actinomycetaceae*	2	3
8.	*Aerococcaceae*	2	3
9.	*Aeromonadaceae*	2	2
10.	*Alcaligenaceae*	6	5
11.	*Alcanivoraceae*	1	4
12.	*Alicyclobacillaceae*	1	1
13.	*Alteromonadaceae*	22	29
14.	*Anammoxales*	4	4
15.	*Anaplasmataceae*	5	5
16.	*Azospirillaceae*	4	4
17.	*Bacillaceae*	49	47
18.	*Bacteroidaceae*	1	3
19.	*Bartonellaceae*	4	4
20.	*Bdellovibrionaceae*	1	1
21.	*Beijerinck/Rhodoplan/Methylocyst*	14	19
22.	*Bifidobacteriaceae*	1	7
23.	*Blattabacteriaceae*	1	1
24.	*Bradyrhizobiaceae*	24	26
25.	*Brevibacteriaceae*	1	1
26.	*Brucellaceae*	2	2
27.	*Burkholderiaceae*	8	7
28.	*Caedibacteraceae*	3	3
29.	*Caldithraceae*	2	2
30.	*Campylobacteraceae*	4	5
31.	*Caryophanaceae*	1	1
32.	*Caulobacteraceae*	11	10
33.	*Cellulomonadaceae*	6	7
34.	*Chlamydiaceae*	1	1
35.	*Chlorobiaceae*	3	3
36.	*Chloroplasts*	16	17
37.	*Chromatiaceae*	9	9

38.	*Clostridiaceae*	41	51
39.	*Comamonadaceae* [b]	45	54
40.	*Coriobacteriaceae*	2	2
41.	*Corynebacteriaceae*	7	7
42.	*Coxiellaceae*	6	6
43.	*Crenotrichaceae*	4	5
44.	*Cryomorphaceae*	ND	1
45.	*Dermabacteraceae*	1	3
46.	*Dermatophilaceae*	1	1
47.	*Desulfoarculaceae*	1	1
48.	*Desulfobacteraceae*	12	12
49.	*Desulfobulbaceae*	8	8
50.	*Desulfohalobiaceae*	1	1
51.	*Desulfomicrobiaceae*	2	2
52.	*Desulfovibrionaceae*	7	9
53.	*Desulfurococcaceae*×	ND	1
54.	*Desulfuromonaceae*	2	2
55.	*Dictyoglomaceae*	1	1
56.	*Dietziaceae*	ND	2
57.	*Ectothiorhodospiraceae*	7	8
58.	*Enterobacteriaceae*	21	45
59.	*Enterococcaceae*	6	7
60.	*Erysipelotrichaceae*	4	4
61.	*Eubacteriaceae*	1	1
62.	*Flammeovirgaceae*	1	1
63.	*Flavobacteriaceae*	27	18
64.	*Flexibacteraceae*	12	11
65.	*Francisellaceae*	1	1
66.	*Frankiaceae*	1	2
67.	*Geobacteraceae*	3	2
68.	*Gordoniaceae*	3	5
69.	*Halobacillaceae*	3	4
70.	*Halomonadaceae*	3	4
71.	*Halothiobacillaceae*	1	5
72.	*Helicobacteraceae*	23	23
73.	*Hydrogenophilaceae*	2	2
74.	*Hydrogenothermaceae*	2	2
75.	*Hyphomicrobiaceae*	13	14
76.	*Hyphomonadaceae*	1	1
77.	*Kineosporiaceae*	3	4
78.	*Lachnospiraceae*	39	39
79.	*Lactobacillaceae*	4	10
80.	*Legionellaceae*	4	3
81.	*Leptospiraceae*	ND	2
82.	*Magnetospirillaceae*	1	1

83.	*Methanosarcinaceae*	ND	1
84.	*Methylobacteriaceae*	2	3
85.	*Methylococcaceae*	6	8
86.	*Methylophilaceae*	1	1
87.	*Microbacteriaceae*	12	14
88.	*Micrococcaceae*	11	12
89.	*Micromonosporaceae*	13	15
90.	*Microthrixineae*	1	1
91.	*Moraxellaceae*	8	8
92.	*Mycobacteriaceae*	17	19
93.	*Mycoplasmataceae*	1	2
94.	*Myxococcaceae*	ND	5
95.	*Neisseriaceae*	5	15
96.	*Nitrosomonadaceae*	13	1
97.	*Nitrospinaceae*	1	10
98.	*Nitrospiraceae*	10	15
99.	*Nocardiaceae*	9	3
100.	*Nocardioidaceae*	1	2
101.	*Oceanospirillaceae*	1	2
102.	*Oxalobacteraceae*	10	12
103.	*Paenibacillaceae*	6	6
104.	*Parachlamydiaceae*	1	1
105.	*Pasteurellaceae*	2	2
106.	*Peptococc/Acidaminococc*	11	11
107.	*Peptostreptococcaceae*	21	23
108.	*Phyllobacteriaceae*	10	11
109.	*Pirellulae*	8	5
110.	*Piscirickettsiaceae*	4	3
111.	*Planctomycetaceae*	2	2
112.	*Polyangiaceae*	15	14
113.	*Porphyromonadaceae*	1	5
114.	*Prevotellaceae*	1	2
115.	*Promicromonosporaceae*	2	2
116.	*Pseudoalteromonadaceae*	2	2
117.	*Pseudomonadaceae*	30	29
118.	*Pseudonocardiaceae*	10	6
119.	*Ralstoniaceae*	4	4
120.	*Rhizobiaceae*	16	18
121.	*Rhodobacteraceae* [a]	53	35
122.	*Rhodobiaceae*	1	1
123.	*Rhodocyclaceae*	16	13
124.	*Rickettsiaceae*	2	3
125.	*Rikenellaceae*	1	1
126.	*Roseococcaceae*	1	1
127.	*Rubrobacteraceae*	6	5

128.	*Saccharospirillaceae*	1	1
129.	*SAR11*	1	ND
130.	*Shewanellaceae*	1	1
131.	*Sphingobacteriaceae*	4	4
132.	*Sphingomonadaceae*	24	37
133.	*Spirochaetaceae*	24	33
134.	*Sporichthyaceae*	ND	2
135.	*Sporolactobacillaceae*	1	2
136.	*Staphylococcaceae*	3	4
137.	*Streptococcaceae*	7	8
138.	*Streptomycetaceae*	14	15
139.	*Streptosporangiaceae*	2	4
140.	*Succinivibrionaceae*	1	ND
141.	*Syntrophaceae*	3	5
142.	*Syntrophobacteraceae*	9	9
143.	*Syntrophomonadaceae*	4	4
144.	*Thermoactinomycetaceae*	1	2
145.	*Thermodesulfobacteriaceae*	1	1
146.	*Thermomonosporaceae*	2	1
147.	*Thermotogaceae*	1	1
148.	*Thiotrichaceae*	8	5
149.	Unclassified[¶]	434	477
150.	*Verrucomicrobia subdivision 3*	2	ND
151.	*Verrucomicrobia subdivision 5*	3	4
152.	*Verrucomicrobia subdivision 7*	3	3
153.	*Verrucomicrobiaceae*	5	5
154.	*Vibrionaceae*	ND	3
155.	*Xanthobacteraceae*	2	3
156.	*Xanthomonadaceae*	10	10
157.	*Xiphinematobacteraceae*	1	1

A total of 1511 and 1678 OTUs found at the Ross and Winze sites respectively were distributed in 149 and 154 families.

[¶] A total of 434 and 477 OTUs in the Ross and Winze sites, respectively could not be assigned to any known family and were considered unclassified.

[a] Most abundant family in the Ross site.

[b] Most abundant family in the Winze site.

× Families belonging to kingdom *Archaea.*
ND-not detected

Supp. Genera Table 4: Bacterial and Archael genera retrieved on PhyloChips from Ross and Winze sites

Representative organisms of the OTUs detected on PhyloChips	Ross site	Winze site
Methanosarcina baltica str. GS1	-	+
hydrothermal vent clone VC2.1 Arc13	-	-
hot spring clone SUBT-14	+	+
hydrothermal vent clone pIVWA11	-	+
soil clone SCA11	+	-
hot spring clone env.OPS7	+	+
Sulfurihydrogenibium azorense	+	+
Coprothermobacter sp. str. Dex80-3	+	+
Thermosipho sp. str. MV1063	+	+
Geothermobacterium ferrireducens	+	+
Antarctic cryptoendolith clone FBP471	+	+
sludge clone SBR2022	+	+
Green non-sulfur isolate str. B1-5	+	+
forest soil clone DUNssu055 (-2B) (OTU#087)	+	+
DCP-dechlorinating consortium clone SHA-21	+	+
anaerobic bioreactor clone SHD-71	+	+
hydrothermal vent polychaete mucous clone P. palm C 37	+	+
Thermus sp. str. C4	+	+
Vulcanithermus mediatlanticus str. TR	+	+
hypersaline pond clone LA7-B27N	+	+
geothermal clone ST01-SN3H	+	+
forested wetland clone FW68	+	+
sludge clone SBRA136	+	+
sludge clone SBR1039	-	+
4MB-degrading consortium clone UASB_TL26	+	+
uranium mining waste pile clone JG37-AG-131 sp.	+	+
Great Artesian Basin clone G19	+	+
lab-scale sludge clone SBR1108	+	-
uranium tailings soil clone Sh765B-AG-45	+	+
uranium mining waste clone JG34-KF-252	+	+
acid mine drainage clone BA29	-	+
forested wetland clone FW114	+	+
mercury and PCB contaminated saltmarsh sediment clone LCP-6 LCP-6	+	+
forested wetland clone FW19	+	+
forested wetland clone FW5	+	+
ground water deep-well injection disposal site radioactive wastes Tomsk-7 clone S15A-MN30 bacterium	+	+
forested wetland clone FW118	+	+
Elbe river clone DEV055	+	+
anoxic marine sediment clone LD1-PA34	+	+
Elbe river clone DEV045	+	+
anoxic marine sediment clone LD1-PB20	+	+
anoxic marine sediment clone LD1-PB12	+	+

anoxic marine sediment clone LD1-PB1	+	+
anoxic marine sediment clone LD1-PA20	+	+
anoxic marine sediment clone LD1-PA50	-	+
Guaymas Basin hydrothermal sediment clone a2b018	+	+
Mono lake clone ML316M-1	+	+
Fucophilus fucoidanolyticus str. SI-1234	+	+
coal effluent wetland clone RCP2-6	+	+
Opitutus sp. str. SA-9	+	+
sludge clone H2	+	+
forested wetland clone FW49	+	-
coal effluent wetland clone FW4	+	-
Akkermansia muciniphila	+	+
hydrothermal vent polychaete mucous clone P. palm C 85	+	+
Candidatus Xiphinematobacter brevicolli	+	+
termite gut homogenate clone Rs-P07 bacterium	+	+
termite gut homogenate clone Rs-D89	+	+
UASB reactor granular sludge clone PD-UASB-13 G+C	+	+
Flexistipes sp. str. E3_33	+	+
terephthalate-degrading consortium clone TA19	+	+
uranium mining waste pile soil sample clone JG30-KF-CM45	+	+
Synergistes sp. P1 str. P4G_18	+	+
hot spring clone OPB72	+	+
DCP-dechlorinating consortium clone SHA-1	+	+
polluted aquifer clone BVC56	+	+
CB-contaminated groundwater clone GOUTB15	+	+
uranium mining mill tailing clone GR-296.II.52 GR-296.I.52	+	+
fjord ikaite column clone un-c23	+	+
Ferribacter thermoautotrophicus	+	+
penguin droppings sediments clone KD1-1	+	+
hot spring clone OPB25	+	+
soil clone PBS-25	+	+
termite gut homogenate clone Rs-D43 group	+	+
thermal spring mat clone O1aA90	+	+
Guaymas Basin hydrothermal sediment clone a2b010	+	+
DCP-dechlorinating consortium clone SHA-124	+	-
termite gut homogenate clone Rs-H93 group	+	+
termite gut homogenate clone Rs-D95 group	-	+
marine sediment above hydrate ridge clone Hyd24-44 sp.	+	+
forest soil clone S0134	+	+
marine sediment clone Sva0515	+	+
uranium mining waste pile clone JG37-AG-81 sp.	+	+
uranium mining waste pile clone JG34-KF-153	+	+
forested wetland clone FW144	+	+
uranium mill tailings soil sample clone GuBH2-AG-47 sp.	+	+
marine sediment above hydrate ridge clone Hyd24-32	+	+
uranium mining waste pile clone JG37-AG-36	+	+
uranium mill tailings soil sample clone GuBH2-AD-9 sp.	+	+
trichloroethene-contaminated site clone FTLM205 proteobacterium	+	+

trichloroethene-contaminated site clone FTLM5 bacterium	-	+
rumen clone BS5	+	+
anaerobic VC-degrading enrichment clone VC47 bacterium	+	+
soil metagenomic library clone 17F9	+	+
activated sludge clone 2951	+	+
soil clone RB27	-	+
Mammoth cave clone CCM15a	+	+
soil clone 23k22	-	+
soil clone 576-2	-	+
Holophaga/Acidobacterium phylum clone iii1-15	+	+
bioreactor clone mle1-25	+	+
Mammoth cave clone CCM8b	+	+
benzoate-degrading consortium clone BA059	+	+
soil sample uranium mining waste pile near town Johanngeorgenstadt clone JG36-TzT-10	+	+
uranium mining waste pile clone JG34-KF-27	+	+
soil clone C112	+	+
soil sample uranium mining waste pile near town Johanngeorgenstadt clone JG36-TzT-202 bacterium	+	+
uranium mining waste pile clone JG37-AG-112 sp.	+	+
uranium mining waste pile clone JG37-AG-29 sp.	+	+
uranium mining waste pile clone JG37-AG-73 sp.	+	+
soil clone BAC-14A1	+	+
soil clone DA023	+	+
soil clone RB24	+	+
uranium mill tailings soil sample clone GuBH2-AD-16 sp.	+	+
Holophaga/Acidobacterium phylum clone ii3-12	-	+
heavy metal-contaminated soil clone a13114	+	+
Holophaga/Acidobacterium phylum clone 32-10	+	+
uranium mining waste pile clone JG34-KF-135	+	+
uranium mining waste pile clone JG37-AG-31 sp.	+	+
uranium mining waste pile clone JG37-AG-145 sp.	+	+
soil sample uranium mining waste pile near town Johanngeorgenstadt clone JG36-TzT-200 bacterium	+	+
uranium mining waste pile clone JG37-AG-117 sp.	+	+
termite gut homogenate clone Rs-D38 bacterium	-	+
termite gut homogenate clone Rs-D44 bacterium	+	+
trichloroethene-contaminated site clone FTLpost3 bacterium	+	+
Mono Lake at depth 35 m station 6 July 2000 clone ML635J-40 bacterium	+	+
SHA-25 clone	+	+
marine sediment above hydrate ridge clone Hyd-B2-1 bacterium	+	+
marine? clone KD3-17	+	+
Mono Lake at depth 35 m station 6 July 2000 clone ML635J-15 bacterium	+	+
DCP-dechlorinating consortium clone SHA-94	-	+
hydrothermal vent polychaete mucous clone P. palm A 53	+	+
penguin droppings sediments clone KD1-125	+	+
anoxic bulk soil flooded rice microcosm clone BSV73	+	+
chlorobenzene-degrading consortium clone IIIB-1	+	+
corneal ulcer clone E1-K9	+	+

swine intestine clone p-987-s962-5	-	+
Bacteroides distasonis	-	+
Dysgonomonas wimpennyi str. ANFA2	+	+
sphagnum peat bog clone 26-4b2	-	+
mouse feces clone L11-6	-	+
cow rumen clone BF24	+	+
cow rumen clone BE14	-	+
rumen clone F24-B03	+	+
mouse feces clone F8	-	+
Crocinitomix catalasitica str. IFO 15977	-	+
Blattabacterium species	+	+
Delaware River estuary clone 1G12	+	+
patient's bronchoalveolar lavage isolate str. MDA2507 sp.	+	-
Flavobacterium frigoris str. LMG 21471	+	+
Arctic sea ice ARK10159	+	+
ground water deep-well injection disposal site radioactive wastes Tomsk-7 clone S15A-MN27 bacterium	+	+
Flavobacterium hibernum str. ATCC51468	+	-
Flavobacterium aquatile	+	+
Tenacibaculum maritimum str. IFO 15946	+	+
marine sediment above hydrate ridge clone Hyd24-41 bacterium	+	-
Tenacibaculum ovolyticum str. IAM14318	+	+
Riftia pachyptila's tube clone R103-B20	+	+
Capnocytophaga sp. str. ChDC OS43	+	-
Cytophaga sp. I-545	+	+
Aequorivita antarctica str. QSSC9-14	+	-
Bacteroidetes Ko706	-	+
Cytophaga sp. str. MBIC04693	+	-
Flavobacterium sp. str. V4.MS.29 = MM_2747	+	+
Cytophaga uliginosa	+	+
Arctic sea ice ARK10004	-	+
bacterioplankton clone AEGEAN_179	+	-
marine bacterioplankton clone MB11E04	+	-
Psychroserpens burtonensis str. S2-64	+	-
acidic forest soil clone UC1	+	+
marine? clone KD3-67	+	+
DCP-dechlorinating consortium clone SHA-5	+	+
marine sediment above hydrate ridge clone Hyd89-72 bacterium	+	+
fruiting body Pleurotus eryngii clone PE01	+	+
Mono Lake at depth 35 m station 6 July 2000 clone ML635J-56	+	+
hydrothermal vent polychaete mucous clone P. palm C/A 20	+	+
temperate estuarine mud clone KM02	+	+
Pedobacter sp. An13	-	+
crevicular epithelial cells clone AZ123	+	+
activated sludge foam clone 47	+	+
Sphingobacteriaceae str. Ellin160	+	+
municipal wastewater treatment bioreactor isolate str. CAGY10	+	+
Toolik Lake main station at 3 m depth clone TLM11/TLMdgge04	+	+
Sphingobacterium heparinum	+	-

Flexibacter sancti str. IFO 16034	-	+
Austria: Lake Gossenkoellesee clone GKS2-106 GKS2-106	+	-
anaerobic VC-degrading enrichment clone VC10 bacterium	-	+
Flexibacter japonensis str. IFO 16041	+	+
Cilia- respiratory isolate str. 243-54	+	+
Haliscomenobacter hydrossis	+	+
Cytophaga sp. I-1787	+	+
CFB group clone ML615J-4	+	+
Microscilla arenaria str. IFO 15982	+	+
Cyclobacterium marinum str. DSM 745	+	-
Hongiella mannitolivorans str. IMSNU 14012 JC2050	+	+
penguin droppings sediments clone KD6-118	+	+
Hymenobacter group clone KL-59-7-9	-	+
Hymenobacter sp. str. NS/50	+	-
Flexibacter flexilis subsp. pelliculosus str. IFO 16028 subsp.	+	+
Arctic sea ice cryoconite clone ARKCRY-50	+	+
EBPR sludge lab scale clone HP1A92	-	+
travertine hot spring clone SM1C04	+	+
Flexibacter roseolus str. IFO 16030	+	+
Saltmarsh mud clone K-790	+	+
Mammoth cave clone CCM9b	+	+
hydrothermal vent polychaete mucous clone P. palm A 12	+	+
DCP-dechlorinating consortium clone SHA-83	+	+
sludge clone A12b	+	+
Chlorobium ferrooxidans DSM 13031 str. KofoX	+	+
sewage sludge clone	-	+
benzene-degrading nitrate-reducing consortium clone Cart-N3 bacterium	+	+
Chlorobium phaeovibrioides str. 2631	+	+
Chlorobium limicola str. M1	+	+
Caldilinea aerophila	+	-
DCP-dechlorinating consortium clone SHD-231	+	+
mixed genomic activated sludge clone SBR2037	+	+
uranium mining waste pile clone JG34-KF-221	+	+
DCP-dechlorinating consortium clone SHA-27	+	+
benzene-contaminated groundwater clone ZZ14AC19	+	+
forest soil clone C043	+	+
thermophilic UASB granular sludge isolate str. IMO-1 bacterium	-	+
DCP-dechlorinating consortium clone SHA-36	+	+
anaerobic bioreactor clone SHD-238	+	+
sediments collected at Charon's Cascade near Echo River October 2000 clone CCD21	+	+
forest soil clone S0208	+	+
DCP-dechlorinating consortium clone SHA-8	+	+
DCP-dechlorinating consortium clone SHA-147	+	+
travertine hot spring clone SM1D10	+	+
DCP-dechlorinating consortium clone SHA-2	+	+
temperate estuarine mud clone KM87	+	+
aerobic basin clone CY0ARA032A03	+	+
anoxic basin clone CY0ARA028B09	+	+

aerobic basin clone CY0ARA026G04	+	+
USA: Colorado Fort collins Horsetooth Reservoir clone HT2F11	+	+
aerobic basin clone CY0ARA025E11	+	+
anoxic marine sediment clone LD1-PA40	+	-
anaerobic digester clone CY0ARA030F07	+	-
Pirellula sp. str. ACM 3181	+	+
anoxic basin clone CY0ARA027E04	+	-
DCP-dechlorinating consortium clone SHA-43	+	-
anoxic basin clone CY0ARA028C04	+	+
anoxic basin clone CY0ARA027D01	+	+
Crater Lake clone CL500-15	+	+
neutral pH mine biofilm clone 44a-B1-34	+	+
Chlamydophila pneumoniae str. AR39	+	+
Rumen isolate str. YS2	-	+
termite gut homogenate clone Rs-H34	+	+
Arthrospira platensis str. IAM M-135	-	+
Oscillatoria sancta str. PCC 7515	+	+
Lyngbya aestuarii str. PCC 7419	-	+
Anabaena augstumalis 'SCHMIDKE JAHNKE/4a' str. SCMIDKE JAHNKE/4a	-	+
Chlorogloeopsis fritschii str. PCC 6912	+	+
Hapalosiphon welwitschii	+	+
Anabaena circinalis str. AWQC150A	-	+
Nodularia sphaerocarpa str. UTEX B 2093	+	+
Nodularia spumigena str. PCC73104	-	+
Scytonema sp. str. IAM M-262	-	+
Cyanospira rippkae str. PCC 9501	-	+
Anabaena variabilis str. IAM M-204	-	+
Spirulina subsalsa str. FACHB351	+	+
silica sinter depositing geothermal power station discharge drain clone ST01-SN2C	+	+
Synechococcus sp. str. UH7	+	+
Acaryochloris marina str. MBIC11017	+	+
Oscillatoria sp	+	+
LPP-group cyanobacterium isolate str. QSSC5cya QSSC5cya	+	+
Oscillatoria neglecta str. M-82	+	+
Plectonema sp. str. F3	+	+
lichen-dominated Antarctic cryptoendolithic community clone FBP403	+	+
sponge clone TK09	-	+
Synechococcus sp. str. PCC 7502	-	+
Cape Hatteras picoplankton clone OM164	+	+
Skeletonema pseudocostatum str. CSIRO CS-76	+	+
Toolik Lake main station at 3 m depth clone TLM14	+	+
travertine hot spring clone SM2B11	+	+
Cape Hatteras picoplankton clone OM270	-	+
Emiliania huxleyi str. Plymouth Marine Laborator PML 92	+	+
Cyanidium caldarium str. 14-1-1	+	+
plastid clone ML310M-37	-	+
Euglena tripteris str. UW OB	+	+
Lepocinclis fusiformis str. ACOI 1025	+	+

Adiantum pedatum	+	+
Calypogeia muelleriana	+	+
Mitrastema yamamotoi	+	+
Solanum nigrum	+	+
Epifagus virginiana -- chloroplast	+	+
Pisum sativum -- chloroplast	+	+
Cycas revoluta	+	+
soil clone PBS-II-1	+	-
bacterioplankton clone ZA3648c	+	+
Sargasso Sea	-	+
anaerobic benzene-degrading clone Cart-N4	+	+
Solibacter usitatus Ellin6076	+	+
TCE-contaminated site clone FTL227	+	+
uranium mining waste pile clone JG37-AG-39 sp.	+	+
Great Artesian Basin clone B27	+	+
Great Artesian Basin clone B11	+	-
DCP-dechlorinating consortium clone SHA-18	+	+
soil clone RB41	+	+
forested wetland clone FW45	+	+
soil sample uranium mining waste pile near town Johanngeorgenstadt clone JG36-TzT-77 bacterium	+	+
soil isolate Ellin337	+	+
forested wetland clone FW47	+	+
PCE-contaminated site clone CLi114	+	+
grassland soil clone DA052	+	+
PCB-polluted soil clone WD228	+	+
soil clone UA2	+	+
Acidobacterium capsulatum	+	+
soil sample uranium mining waste pile near town Johanngeorgenstadt clone JG36-TzT-31 bacterium	+	+
acid mine drainage clone TRB82	+	+
PCE-contaminated site clone CLs73	+	+
PCB-polluted soil clone WD217	+	+
coal effluent wetland clone FW92	+	+
sphagnum peat bog clone K-5b10	+	+
Spirochaeta sp. str. BHI80-158	+	+
termite gut homogenate clone Rs-B68 sp.	-	+
Mono Lake at depth 23 m station 6 July 2000 clone ML623J-23 bacterium	+	-
spirochete clone ML320J-13	+	+
Spironema culicis str. BR91	+	+
Treponema sp. str. 7CPL208	+	+
Treponema sp	+	+
Treponema sp. str. III:C:BA213	+	+
termite gut clone NkS34	+	+
termite gut homogenate clone Rs-C47 sp.	-	+
forested wetland clone RCP1-96	+	+
termite gut clone NkS-Ste2	-	+
termite gut homogenate clone Rs-J42 sp.	-	+
termite gut homogenate clone Rs-B69 sp.	+	+

termite gut clone NkS50	+	+
Mixotricha paradoxa is flagellate hindgut Mastotermes darwiniensis clone mp3 of	-	+
termite gut homogenate clone Rs-D52 sp.	-	+
Treponema primitia str. ZAS-1	+	+
Mixotricha paradoxa is flagellate hindgut Mastotermes darwiniensis clone mp1 of	-	+
termite gut homogenate clone BCf4-14	+	+
termite gut homogenate clone BCf8-03	+	+
termite gut homogenate clone Rs-J58 sp.	+	+
termite hindgut clone mpsp2	+	+
termite gut homogenate clone Rs-J64 sp.	+	+
termite gut homogenate clone BCf10-21	-	+
termite gut clone NkS39	+	+
termite gut homogenate clone Rs-A43 sp.	-	+
termite gut clone NkS-Oxy25	+	+
Spirochaeta sp	+	+
Mixotricha paradoxa is flagellate hindgut Mastotermes darwiniensis clone mp4	+	+
termite gut clone NkS7	-	+
TCE-contaminated site clone ccslm226	+	-
termite gut clone NkS83	+	+
termite gut homogenate clone Rs-D46 sp.	-	+
forested wetland clone RCP1-64	+	+
neutral pH mine biofilm clone 44a-B1-48	-	+
Leptospira interrogans serovar Copenhageni str. Fiocruz L1-130	-	+
Rocky Mountain alpine soil clone W2b-8C	+	+
Great Artesian Basin clone B35	+	+
Gluconacetobacter europaeus str. ZIM B028 V3	+	+
Acetobacter pomorum str. LTH2458	+	+
deep-sea sediment clone P_wp0211	-	+
diesel-polluted Bohai Gulf isolate str. M-5 M-5	+	+
Thalassospira lucentensis	-	+
Scrippsiella trochoidea NEPCC 15	+	+
Roseospira thiosulfatophila AT2115	+	-
rhizosphere clone wr0007	-	+
soil isolate Ellin333	-	+
Dechlorospirillum sp. str. SN1	+	+
sphagnum peat bog clone K-5b5	+	+
forested wetland clone RCP2-92	+	+
Anabaena circinalis AWQC118C isolate str. UNSW7	+	+
Mammoth cave clone CCU22	+	+
soil near uranium mill tailings clone KCM-C-45	+	+
Rhodocista pekingensis str. 3-p	+	+
uranium mining waste pile near Johanngeorgenstadt soil clone JG37-AG-102	+	+
acid mine drainage clone ASL45	+	+
Azospirillum species	+	+
Great Artesian Basin clone B79	+	+
Azospirillum sp. str. ASP-1	+	+
Rhodocista sp. AR2107	+	+
Pseudovibrio denitrificans str. DN34	+	+

Mammoth cave clone CCM16b	+	+
peat soil microcosm clone LO13.3	-	+
heavy metal-contaminated soil clone a13111	+	+
Hyphomicrobium facile str. H-526	+	+
Hyphomicrobium aestuarii str. DSM 1564	+	+
uranium mining waste pile clone JG34-KF-416	+	+
Beijerinckia indica	+	+
Azorhizobium caulinodans str. ORS 571	+	+
heavy metal-contaminated soil clone a13115	+	+
Microvirga subterranea str. FaiI4; ATCC BAA-295; DSM 14364	+	+
EBPR sludge lab scale clone HP1B78	-	+
grassland soil clone DA122	-	+
Rhodoplanes sp. str. HA17	+	-
Rhizobiales str. A48	+	+
Thiobacillus sp. str. 104	+	+
Xanthobacter agilis str. SA35	-	+
Blastochloris sulfoviridis str. GN1	+	+
Rhodoplanes elegans str. AS130	+	+
soil isolate Ellin362	+	+
Bosea thiooxidans TJ1	+	+
Mammoth cave clone CCU18	+	+
Mammoth cave clone CCM24a	+	+
denitrifying reactor clone 92	+	+
uranium mining mill tailing clone GR-WP33-3 GR-WP33-3	-	+
heavy metal-contaminated soil clone a13113	+	+
Methylosinus sporium	+	+
sludge clone A20	+	+
Methylosinus trichosporium	+	+
Methylocella palustris str. H4	+	+
acidic forest soil clone UP8	+	+
Mammoth cave clone CCM12a	+	-
13C- extracted 13C-methanol exposed soil clone UP2 proteobacterium	-	+
Methylocella tundrae str. Y1	+	+
uranium mill tailings clone Gitt-KF-194	+	+
soil isolate Ellin340	-	+
Methylobacterium thiocyanatum str. ALL/SCN-P	+	+
Methylobacterium fujisawaense	+	+
Methylobacterium organophilum str. JCM 2833	-	+
Bosea massiliensis str. 63287	+	+
Oligotropha carboxidovorans str. S23	+	+
Afipia clevelandensis	+	+
Nitrobacter hamburgensis str. X14	+	+
Nitrobacter sp. str. KB212	-	+
Rhodopseudomonas palustris str. GH	+	+
Rhodopseudomonas palustris str. ATCC 17001	+	+
Afipia genosp. 4 str. G3644	+	+
Rhodopseudomonas rhenobacensis str. Klemme Rb	+	+
Bradyrhizobium japonicum HA1	+	+

Bradyrhizobium japonicum str. USDA 38	+	+
Bradyrhizobium japonicum str. DASA37026	-	+
Bradyrhizobium elkanii str. USDA 76	+	+
heavy metal-contaminated soil clone a13131	+	+
Bradyrhizobium str. YB2	+	+
Afipia genosp. 2 str. G4438	+	+
ground water deep-well injection disposal site radioactive wastes Tomsk-7 clone S15A-MN96 proteobacterium	+	+
Bradyrhizobium sp. str. 2FB3	+	-
Afipia genosp. 10 str. G8996	+	+
Bradyrhizobium elkanii str. SEMIA 6028	+	+
Bradyrhizobium sp. str. KKI14	+	+
Bradyrhizobium japonicum SD5	+	+
Bradyrhizobium japonicum str. IAM 12608	+	+
temperate estuarine mud clone HC65	+	+
Mesorhizobium mediterraneum str. PECA20	+	+
Roseospirillum parvum str. 930I	+	+
hydrocarbon-degrading consortium clone 4-Org2-22	+	+
Phyllobacterium trifolii str. PETP02	+	+
marine bacterioplankton clone MB13F01	+	+
lake microbial mat isolate str. R-9219	+	+
Ahrensia kielensis str. IAM12618	+	+
bacterioplankton clone AEGEAN_108	+	+
Phyllobacterium myrsinacearum HM35	+	+
Aminobacter aminovorans str. DSM7048T	+	+
Pseudaminobacter salicylatoxidans str. KTC001	+	+
Waste-gas biofilter clone BIwii1	+	+
Ochrobactrum anthropi str. ESC1	+	+
Mycoplana dimorpha str. IAM 13154	+	+
soil isolate Ellin332	+	+
Shinella zoogloeoides str. ATCC 19623	+	+
Sinorhizobium fredii str. ATCC35423	+	+
Sinorhizobium meliloti str. 1021	-	+
Ensifer adhaerens str. LMG 20582	+	+
hydrocarbon-degrading consortium clone 4-Org1-36	+	+
Pleomorphomonas oryzae str. B-32	+	+
marine isolate JP57	+	+
Rhizobium giardinii str. H152	+	+
India: Himalayas Kaza Spiti Valley Cold Desert isolate str. Kaza-35 Kaza-35	+	+
Rhizobium tropici str. LMG 9517	+	+
Rhizobium mongolense str. USDA 1832	+	+
Rhizobium gallicum str. FL27	+	+
sludge clone H6	+	+
Rhizobium etli str. USDA 2667 ATCC 14483 SEMIA 043	+	+
Rhizobium leguminosarum bv. viciae str. USDA 2508	+	+
termite gut homogenate clone Rs-D84 proteobacterium	+	+
uranium mining waste pile clone JG34-KF-245 proteobacterium	+	+
termite gut homogenate clone Rs-B50 proteobacterium	+	+
PCE-contaminated site clone CLi8	+	+

Mammoth cave clone CCM21a	+	+
Agrobacterium tumefaciens TG14	+	+
Rhizobium sp. str. SH19312	+	+
Agrobacterium tumefaciens str. C58 Cereon	+	+
Agrobacterium tumefaciens C4	+	+
Rhizobium huautlense str. SO2 ()	+	+
Bartonella schoenbuchensis str. R1	+	+
Mariana trough hydrothermal vent water 0.2micro-m filterable fraction clone MT-NB25	+	+
aortic heart valve patient with endocarditis clone v9	+	+
Bartonella quintana str. Toulouse	+	+
Bartonella henselae str. Houston-1	+	+
Caulobacter sp. str. FWC38	+	+
Brevundimonas sp. str. MCS17	+	-
Brevundimonas intermedia str. MBIC2712 ATCC15262	+	+
Brevundimonas vesicularis str. IAM 12105T	+	+
Brevundimonas diminuta str. DSM 1635	+	+
Brevundimonas diminuta str. IAM 12691T	+	+
Brevundimonas bacteroides str. CB7	+	+
Brevundimonas subvibrioides str. CB81	+	+
Brevundimonas sp. str. FWC40	+	+
marine clone Arctic96A-1	+	+
Roseobacter clone NAC11-3	+	+
Sulfitobacter sp. PIC-72	+	+
Arctic sea ice ARK10013	+	+
Loktanella vestfoldensis str. LMG 22003	+	+
Antarctic seawater isolate str. R7706	+	+
Roseobacter sp. str. KT0202a	+	+
Scrippsiella trochoidea NEPCC 15	+	+
Sulfitobacter sp. BIO-11	+	+
Prionitis lanceolata gall symbiont	+	+
Roseobacter sp. str. KT0917	+	-
Arctic sea ice ARK10226	+	+
Roseobacter sp. str. ANT9274	+	+
coastal sediment clone	+	-
Arctic sea ice ARK10055	+	+
Leisingera methylohalidivorans str. MB2	+	+
Rhodobacter group clone LA1-B32N	-	+
Ruegeria atlantica str. WNA2	+	-
Mono Lake at depth 35 m station 6 July 2000 clone ML635J-2 proteobacterium	+	+
Roseobacter sp. str. ARK9990	+	-
Methylarcula sp. BIO-24	+	+
unialgal raphidophyte Chattonella marina isolate str. Fl90-32 bacterium	+	+
Roseobacter sp. 4318-8/1	+	+
Ruegeria atlantica str. IAM14464	+	-
Loktanella salsilacus str. LMG 22000	+	-
Paracoccus pantotrophus str. TUT1022	+	+
Paracoccus yeei str. G6446	+	-
Paracoccus alcaliphilus str. JCM 7364	+	+

Paracoccus carotinifaciens str. E-396	+	+
Paracoccus solventivorans str. ATCC 700252	+	-
Rhodobacter sp. AP-10	+	+
Gram-negative MM 1	+	+
Pseudorhodobacter ferrugineus str. IAM12616	+	+
Colored moderately thermophilic paper-machine biofilms paper machine biofilm	+	+
deep sea sediment clone NKB7	+	+
non-EBPR sludge clone SBRT155	+	+
lichen-dominated Antarctic cryptoendolithic community clone FBP492 proteobacterium	+	-
sludge clone A6	+	-
Rhodobacter sphaeroides str. 2.4.1	+	+
Rhodobacter massiliensis str. Framboise	+	-
Rhodobacter capsulatus str. B10	+	-
Jannaschia sp. DFL-38	+	-
bacterioplankton clone ZA2526c	-	+
Rhodovulum sp. CP-10	+	-
sponge clone TK03	+	+
Rhodovulum strictum str. MB-G2	+	-
Maricaulis maris str. ATCC 15269	+	+
Maricaulis indicus str. MCS26	+	+
travertine hot spring clone SM2C07	+	+
Scrippsiella trochoidea NEPCC 15	+	+
Hyphomonas johnsonii str. MHS-2	+	-
Candidatus Pelagibacter ubique str. HTCC1002	+	+
marine clone Arctic95D-8	+	-
bacterioplankton clone AEGEAN_233	-	+
marine clone Arctic96B-6	+	+
marine bacterioplankton clone MB12A07	+	-
ferromanganous micronodule clone MND8	+	+
periodontal pocket clone 10B6	+	+
Rickettsia rickettsii str. Sawtooth	+	+
termite gut homogenate clone Rs-B60 proteobacterium	+	+
termite gut homogenate clone Rs-M62 proteobacterium	+	+
Rickettsia bellii str. strains 369-C and G2D42	+	+
Anaplasma bovis	-	+
Wolbachia pipientis	+	+
Wolbachia sp	+	+
Wolbachia sp. Dlem16SWol	+	+
coal effluent wetland clone RCP124	+	+
Rhinocyllus conicus endosymbiont	+	-
Wolbachia pipientis	+	+
Sphingobium chungbukense str. DJ77	+	+
Sphingobium yanoikuyae str. GIFU9882	+	+
Afipia genosp. 13 str. G8991	+	+
Sphingomonas sp. str. SAFR-010	+	+
isolate str. '#33 orange'	+	+
Sphingomonas echinoides	-	+
Sphingomonas sp. str. SAFR-027	+	+

Sphingomonas sp. V1 str. V21	+	+
Sphingomonas paucimobilis str. GIFU2395	+	+
Kaistobacter koreensis str. PB229	-	+
heavy metal-contaminated soil clone a13102	-	+
Sphingomonas asaccharolytica str. IFO 10564-T	+	+
pea aphid symbiont clone APe4_19	+	+
travertine hot spring clone SM2B06	+	+
soil clone 768-2	-	+
marine clone Arctic95C-5	+	+
Sphingomonas sp. str. B9	+	+
Sphingopyxis flavimaris str. SW-151	+	+
lichen-dominated Antarctic cryptoendolithic community clone FBP255 proteobacterium	+	+
activated sludge clone 1958	-	+
Novosphingobium sp. str. K16	+	+
Novosphingobium subarcticum LH128	+	+
Novosphingobium tardaugens str. ARI-1	-	+
Sphingomonas sp. str. IW3	-	+
Novosphingobium subterraneum str. IFO 16086	-	+
Novosphingobium sp. str. J30	-	+
Novosphingobium stygium str. IFO 16085	+	+
Japan:NaganoLake Suwa isolate str. 7CY	+	+
Sphingopyxis chilensis str. S37	-	+
Sphingopyxis witflariensis str. W-50	+	+
Porphyrobacter tepidarius str. OK5APO	+	+
Porphyrobacter tepidarius str. DSM 10594	+	+
Erythrobacter sp. str. AS-45	-	+
str. MBIC3035 PC4	+	+
Aquaspirillum serpens str. IAM 13944	+	+
Aquaspirillum putridiconchylium str. IAM 14964	+	+
Neisseria sp. str. CCUG 46910	+	+
Nitrosovibrio sp. str. RY6A	-	+
Nitrosospira sp. str. TYM9	+	+
sample taken upstream landfill clone BVC77 landfill	+	-
Nitrosospira briensis str. Nsp10	+	+
Nitrosospira multiformis	+	+
Nitrosomonas sp. str. Nm86	+	+
Nitrosomonas sp. str. Nm59	+	+
freshwater clone PRD01a011B	+	+
Nitrosomonas europaea str. ATCC 19718	+	+
Nitrosomonas eutropha str. Nm57	+	+
travertine hot spring clone SM1E12	+	-
silica sinter depositing geothermal power station discharge drain clone ST01-SN1D proteobacterium	-	+
EBPR sludge clone SA34	+	-
agricultural soil clone SC-I-71	+	+
iron-oxidizing acidophile isolate m-1	+	-
Uranium mill tailings soil sample clone Sh765B-TzT-132 proteobacterium	+	+
Zoogloea ramigera str. ATCC 19544 (T)	+	+

sludge clone H13	+	+
EBPR sludge lab scale clone HP1A03	+	+
Thauera aromatica str. LG356	+	+
uranium mining mill tailing clone GR-WP33-36 GR-WP33-36	+	+
uranium mining waste pile near Johanngeorgenstadt soil clone JG37-AG-35	+	+
termite gut homogenate clone Rs-B77 proteobacterium	+	+
Azoarcus tolulyticus str. 2FB6	+	-
P+ sludge clone GC24	+	+
Thiobacillus aquaesulis	+	+
penguin droppings sediments clone KD1-79	+	+
swine intestine clone p-861-a5	+	+
Alcaligenes defragrans str. PD-19	+	+
Alcaligenes faecalis str. M3A	+	+
Achromobacter subsp. denitrificans str. DSM 30026 (T)	+	+
Waste-gas biofilter clone BIfciii38	+	-
Alcaligenes sp. str. VKM B-2263 dcm6	+	+
Waste-gas biofilter clone BIfdi44	+	+
Comamonas terrigena str. IAM 12052T	+	-
EBPR sludge lab scale clone HP1B33	+	+
Comamonas testosteroni	-	+
Comamonas testosteroni str. SMCC B329	+	+
Guaymas Basin hydrothermal sediment clone a2b013	+	+
oral periodontitis clone EW086	+	+
Comamonas sp. str. PJ712	+	+
Hydrogenophaga sp. str. ATCC BAA-306 YED1-18 ATCC	+	+
travertine hot spring clone SM1E01	+	+
Hydrogenophaga taeniospiralis str. ATCC 49743	+	+
Mars Odyssey Orbiter and encapsulation facility clone T5-1 sp.	+	+
freshwater clone PRD01b009B	+	+
Toolik Lake main station at 3 m depth clone TLM04/TLMdgge03 proteobacterium	-	+
Polaromonas vacuolata str. 34-P	+	+
Toolik Lake main station at 3 m depth clone TLM05/TLMdgge10 proteobacterium	+	+
Polaromonas naphthalenivorans str. CJ2	-	+
Xylophilus ampelinus str. ATCC 33914	+	+
penguin droppings sediments clone KD2-104	-	+
penguin droppings sediments clone KD5-43	+	+
MCB-contaminated groundwater-treating reactor clone RB9C10	+	+
Arctic sea ice ARK10281	+	+
penguin droppings sediments clone KD3-141	-	+
Pseudomonas lanceolata str. ATCC 14669T	+	+
Delftia tsuruhatensis str. AD9	+	+
Anabaena circinalis AWQC118C isolate str. UNSW5	-	+
Variovorax paradoxus	+	+
napthalene-contaminated sediment clone 76	+	+
Variovorax paradoxus str. IAM 12373	+	+
penguin droppings sediments clone KD2-46	-	+
PCB-polluted soil clone WD291	+	+
soil clone	-	+

Hydrogenophaga flava str. DSM 619T	+	+
uranium mill tailings clone Gitt-KF-21	-	+
strain isolate str. rM4	+	+
Variovorax paradoxus TG27	+	+
marine? clone KD1-99	+	+
Acidovorax sp. str. OS-6	+	+
Ottowia thiooxydans str. K11	+	+
hydrocarbon-degrading consortium clone AF1-8	+	+
denitrifying reactor clone 81	+	+
Acidovorax konjaci str. DSM 7481	+	+
Acidovorax delafieldii str. ATCC 17505	+	+
Acidovorax facilis str. CCUG 2113	+	+
Acidovorax avenae subsp. cattleyae str. NCPPB 961 subsp.	+	+
strain isolate str. rJ10	+	+
Acidovorax defluvii str. BSB411	+	+
Aquaspirillum metamorphum str. DSM 1837	+	+
isolate str. A0640	+	+
Rubrivivax gelatinosus str. A3	+	+
Schlegelella sp. str. KB1a	-	+
Limnobacter thiooxidans str. CS-K2	+	+
Leptothrix discophora str. SS-1	+	-
Leptothrix cholodnii str. CCM 1827	+	+
isolate str. A1004	+	-
hydrothermal vent clone VC2.1 Bac29	-	+
Aquabacterium parvum str. B6	+	+
Anoxobacterium dechloraticum	+	+
uranium mill tailings soil sample clone GuBH2-AD-29 proteobacterium	+	+
Burkholderia glathei str. ATCC 29195T	+	+
soil sample uranium mining waste pile near town Johanngeorgenstadt clone JG36-TzT-215 proteobacterium	+	+
Burkholderia sp.	+	+
Burkholderia graminis str. AUS35	+	+
Burkholderia caryophylli str. ATCC 25418	+	+
forested wetland clone FW145	+	+
Elbe River snow isolate Iso18 Iso18_1411	+	+
Burkholderia cepacia LS2.4	+	+
Chitinimonas taiwanensis str. cf	+	+
Burkholderia cepacia	+	+
Herbaspirillum sp. str. NAH4	+	+
uranium mining waste pile clone JG37-AG-125 proteobacterium	+	+
Massilia timonae timone	+	+
Diaphorina citri symbiont	+	+
Paucimonas lemoignei str. ATCC 17989T	+	+
napthalene-contaminated sediment clone 29	-	+
Collimonas fungivorans str. Ter331	+	+
Oxalobacter formigenes str. OXB ovinen rumen	+	+
isolate str. A1020	+	+
Aquaspirillum arcticum str. IAM 14963	+	+
Janthinobacterium agaricidamnosum str. W1r3T	+	+

Herbaspirillum seropedicae str. DSM 6445 ATCC 35892	+	+
2-HNA producing isolate MC13289	-	+
Wautersia basilensis str. DSM 11853	+	+
Wautersia paucula str. LMG 3413	+	+
Cupriavidus necator	+	+
Ralstonia detusculanense str. APF11	+	+
Halorhodospira neutrophila str. SG 3304	+	+
Ectothiorhodospiraceae clone LA7-B9	+	+
hypersaline Mono Lake clone ML110J-5	+	+
Alkalispirillum mobile	+	+
Mono Lake at depth 2 m station 6 July 2000 clone ML602J-47 proteobacterium	-	+
uranium waste soil clone JG30-KF-CM35	+	+
activated sludge clone SBRH10	+	+
Mammoth Cave sediment clone CCD24	+	+
acid mine drainage clone BA11	+	+
Acidithiobacillus ferrooxidans str. D2	+	+
Acidithiobacillus albertensis str. DSM 14366	+	+
Nitrosococcus halophilus	+	-
forested wetland clone RCP2-96	+	+
Nitrosococcus oceanus	+	+
marine sediment clone Limfjorden L8	+	+
Thioploca ingrica	+	-
marine sediment clone Limfjorden L10	+	+
Beggiatoa sp. str. MS-81-1c	+	+
Beggiatoa alba str. B18LD; ATCC 33555	+	+
marine sediment clone Tokyo Bay D	+	-
Allochromatium sp. AT2202	-	+
Thiocapsa litoralis	+	+
deep-sea sediment clone BD1-1	-	+
Chromatiaceae clone LA4-B63N	+	+
Thiorhodovibrio winogradskyi	+	+
Thiococcus sp. AT2204	+	+
Thiorhodovibrio sibirica	+	+
uranium mining waste pile clone JG37-AG-14 proteobacterium	+	+
forested wetland clone RCP2-54	+	+
isolate str. IR	+	+
Acidithiobacillus ferrooxidans str. DSM 2392	+	+
Solemya reidi symbiont 2	+	+
deepest cold-seep area Japan Trench clone JTB35 proteobacterium	+	+
Norway:(Svalbard)Hornsund clone Sva0864	+	+
Selenate-reducing isolate str. KE4OH1	+	+
marine sediment clone B2M54	+	+
f cytometric sorted marine sample subpopulation 3 clone ZD0408 bacterium	+	+
hydrothermal sediment clone AF420367	+	+
inactive deep-sea hydrothermal vent chimneys clone IheB2-13	+	+
marine clone Arctic97C-5	+	+
Lucina nassula gill symbiont	+	+
Codakia orbicularis gill symbiont	-	+

unclassified Lamellibrachia sp. 1 symbiont Lamellibrachia	+	+
Mammoth cave clone CCM19a	+	+
Seepiophila jonesi symbiont	+	+
microbial mat cave sulfidic spring clone LKC3_19.29	+	-
bacterioplankton clone ZA2525c	+	+
inactive deep-sea hydrothermal vent chimneys clone IheB2-31	+	+
Bathymodiolus thermophilus gill symbiont	+	+
sea water isolate str. DBF-MAK	+	+
Cycloclasticus spirillensus str. M4-6	+	-
Methylophaga alcalica str. M39	+	+
Methylophaga sp. str. V4.ME.29 = MM_2343	+	+
Tilapia parasite TPT-541	+	+
uranium waste soil clone JG30a-KF-21	+	+
Halothiobacillus sp.	+	+
Halothiobacillus sp. str. RA13	-	+
Halothiobacillus neapolitanus str. DSM 581	-	+
Halothiobacillus hydrothermalis str. r3	+	+
Halothiobacillus halophilus	-	+
Halothiobacillus sp. str. WJ18	-	+
water 5 m downstream manure clone 35ds5	+	+
hexane degrading biofilter isolate MN 154.3	+	-
Germany:Schlema/Alberoda clone GR-296.I.104 proteobacterium	-	+
Nevskia ramosa	-	+
pea aphid symbiont clone APe4_38	+	+
uranium mining waste pile clone JG37-AG-94 proteobacterium	+	+
Dyemonas todaii str. XD10	+	+
acid mine drainage clone TRA5-3	+	-
Iron oxidising strain ES-1	+	+
Thermomonas fusca str. LMG 21738	+	-
Waste-gas biofilter clone BIyi3	+	+
lodgepole pine rhizosphere soil British Columbia Ministry Forests Long-Term Soil Productivity	+	+
travertine hot spring clone SM1E05	+	+
Xanthomonas axonopodis pv. citri str. MA	+	+
Stenotrophomonas rhizophila str. e-p10	+	+
Stenotrophomonas maltophilia str. LMG 11104	+	+
Legionella steigerwaltii str. ATCC 35302	+	+
Legionella parisiensis	+	-
bacterioplankton clone AEGEAN_234	+	+
Legionella pneumophila str. Paris	+	+
5' clone CHAB-XI-27	+	+
uranium mining waste pile clone KF-JG30-B15 KF-JG30-B15	+	+
Legionella rubrilucens str. ATCC 35304	+	+
North Sea clone KTc0924	+	+
uranium mining waste pile soil sample clone JG30-KF-C15 proteobacterium	+	+
	+	+
Mars Odyssey Orbiter and encapsulation facility clone T5-3	+	+
Methylococcus capsulatus Bath str. ACM 3302 ATCC 33009 NCIBM 1113	+	+
activated sludge clone SBRL2_19	+	+

activated sludge clone SBRQ157	+	+
activated sludge clone SBRL2_40	+	+
coal tar-contaminated groundwater clone 4-25	+	+
Methylobacter whittenburyi str. 3310 NCIMB 11128 ACM 3306	-	+
Methylobacter psychrophilus str. Z-0021	+	+
extracted chamber connected to Ocean Drilling Program site 892b clone 1-27 proteobacterium	+	-
Methylobacter marinus str. A45	+	+
marine sediment above hydrate ridge clone Hyd24-01 proteobacterium	+	+
Chromohalobacter israelensis str. ATCC 43985 T	+	+
Halomonas desiderata str. FB2	+	+
Boston Harbor surface water isolate str. UMB18C UMB18C	-	+
Halomonas sp. SK1	+	+
marine isolate NOR5	+	-
Marinomonas protea	-	+
forested wetland clone FW23	+	+
Alcanivorax sp. str. K3-3 (MBIC 4323)	+	+
North Sea; NOR3 isolate str. KT0221	-	+
Alcanivorax borkumensis str. LE4	-	+
Alcanivorax sp. str. Haw1	-	+
Psychrobacter frigidicola str. DSM 12411	+	+
Moraxella oblonga str. IAM 14971	+	+
Psychrobacter psychrophilus CMS 28	+	+
Alkanindiges hongkongensis str. HKU9	+	+
Acinetobacter junii str. S33	+	+
hydrocarbon-degrading consortium clone AF2-1D	+	+
Acinetobacter tandoii str. 4N13	+	+
Acinetobacter haemolyticus	+	+
Lyrodus pedicellatus symbiont	+	+
Lyrodus pedicellatus symbiont	+	+
Pseudomonas aeruginosa str. #47	+	+
Pseudomonas stutzeri HY-105	+	+
Pseudomonas mendocina str. KR	+	-
Pseudomonas fulva str. IAM 1587	+	+
Pseudomonas sp. str. 2N1-1	+	+
ground water deep-well injection disposal site radioactive wastes Tomsk-7 clone S15A-MN7 proteobacterium	+	+
Pseudomonas monteilii str. CIP 104883	+	+
Pseudomonas cf. monteilii 9	+	+
cf. Pseudomonas sp. clone Llangefni 52	+	+
Pseudomonas sp. str. dcm7B	+	+
Pseudomonas syringae pv. broussonetiae str. KOZ 8101 pv.	+	+
bacterioplankton clone ZA3412c	-	+
Beggiatoa sp. str. AA5A	+	+
Pseudomonas koreensis str. Ps 9-14	+	+
hydrothermal sediment clone AF420370	+	+
Pseudomonas fluorescens str. CHA0	+	+
Pseudomonas syringae pv. theae str. PT1	+	+
Pseudomonas sp. str. AC-167	+	+

Pseudomonas synxantha str. DSM 13080 G	+	+
Pseudomonas sp. B65	+	+
Pseudomonas marginalis str. ATCC 10844T	+	+
Pseudomonas sp. str. NMX	+	-
Pseudomonas putida str. ATCC 17472	+	+
uranium mining mill tailing clone GR-296.II.89 GR-296.II.89	+	+
Pseudomonas extremorientalis str. KMM3447	+	+
Pseudomonas fulgida str. DSM 14938 = LMG 2146 P 515/12	+	+
Pseudomonas tolaasii str. LMG 2342T ()	+	+
Pseudomonas sp. SK-1-3-1	+	+
Pseudomonas psychrophila str. E-3	+	+
silica sinter depositing geothermal power station discharge drain clone ST01-SN4A proteobacterium	-	+
Arctic sea ice ARK10148	+	+
Alteromonadaceae isolate str. LA50	-	+
Marinobacter aquaeolei str. KT02ds19	+	+
Arctic sea ice ARK10244	-	+
Alteromonadaceae isolate str. LA13	+	+
Marinobacter lipolyticus str. SM-19	-	+
Marinobacter sp. str. SBS	+	+
Marinobacter hydrocarbonoclasticus str. ATCC 27132T	+	+
bacterioplankton clone AEGEAN_133	+	+
Arctic sea ice ARK10228	-	+
Arctic deep sea Isolation common chemoorganotrophic oxygen-respiring polar current d 1210	+	+
Marinobacter excellens str. KMM 3809	+	-
Rheinheimera baltica str. OS140 Baltic # 166	+	-
Alishewanella fetalis str. CCUG 30811	+	-
Colwellia maris str. ABE-1	+	+
Colwellia piezophila str. Y223G	+	-
Thalassomonas ganghwensis str. JC2041	+	+
Marine isolate str. GK-2001	+	+
Boston Harbor surface water isolate str. UMB6D UMB6D	+	-
attached marine recovered surface clone 17 proteobacterium	+	+
Arctic pack ice; northern Fram Strait; 80 31.1 N; 01 deg 59.7 min E clone ARKIA-34	-	+
Alteromonas marina str. SW-47	-	+
Arctic seawater isolate str. R9879	+	+
Arctic sea ice ARK10108	+	+
Antarctic pack ice Lasarev Sea Southern Ocean clone ANTXI/4_14-62 sea	-	+
attached marine recovered surface clone 18 proteobacterium	-	+
Alteromonas stellipolaris str. LMG 21861	+	+
sea water isolate str. BP-PH	+	+
Alteromonadaceae clone PH-B55N	+	+
Pseudoalteromonas sp. str. Bdeep-1	+	+
Alteromonas sp. str. NIBH P1M3	+	+
Pseudoalteromonas sp. str. E36	+	+
marine clone Arctic96B-17	+	+
Pseudoalteromonas sp	+	+

Pseudoalteromonas porphyrae str. S2-65	+	+
Pseudoalteromonas sp. str. 05	+	+
Shewanella surugensis str. c959	+	+
Photobacterium leiognathi str. LN101	-	+
Arctic pack ice; northern Fram Strait; 80 31.1 N; 01 deg 59.7 min E clone ARKDMS-58	+	+
Vibrio aestuarianus str. KT0901	-	+
Vibrio aestuarianus str. 01/151	-	+
Anaerobiospirillum sp. str. 3J102	+	-
Aeromonas sp. PAR2A	+	+
Histophilus somni str. CCUG 12839	+	+
Buchnera sp	-	+
USA:New York isolate str. KN4	-	+
Alterococcus agarolyticus str. ADT3; CCRC17102	-	+
intestine Zophobas mori clone	+	+
Salmonella subsp. enterica serovar Waycross str. Swy1 subsp.	-	+
Salmonella typhimurium LT2 str. SGSC1412	-	+
Erwinia chrysanthemi str. 571	-	+
Erwinia chrysanthemi str. ATCC 11663	-	+
Erwinia amylovora str. DSM 30165	-	+
Erwinia amylovora str. BC199(=Ea528)	-	+
Morganella morganii str. AP28	-	+
Morganella morganii str. ATCC35200	+	+
Pectobacterium cypripedii str. ATCC 29267	-	+
Salmonella bongori str. JEO 4162	-	+
Pantoea agglomerans str. A40	-	+
Baumannia cicadellinicola	+	-
Pantoea subsp. stewartii str. GSPB 2626	-	+
Vryburgia amaryllidis symbiont	+	+
Dysmicoccus neobrevipes symbiont	+	+
Amonostherium lichtensioides symbiont	+	+
Baumannia cicadellinicola	+	-
Serratia marcescens subsp. sakuensis str. KRED subsp.	-	+
Buttiauxella warmboldiae str. DSM 9404	-	+
Enterobacter cloacae Nr. 3	-	+
Enterobacteriaceae CF01Ent-1	-	+
Klebsiella oxytoca str. ChDC OS31	-	+
Enterobacter ludwigii str. EN-119 = DSMZ 16688	-	+
Enterobacter intermedius str. JCM1238	-	+
Raoultella planticola 7	-	+
Raoultella planticola str. DR3	-	+
Klebsiella pneumoniae str. ASR1	-	+
Cyphonococcus alpinus symbiont	+	+
Serratia proteamaculans str. DSM 4543	-	+
Serratia entomophila str. DSM 12358	-	+
Aranicola proteolyticus	+	+
Serratia fonticola str. DSM 4576	+	+
Heteropsylla texana symbiont	+	+
Morganella morganii	+	-

Morganella morganii str. JU27	+	-
Photorhabdus asymbiotica str. ATCC 43949	+	-
Hafnia alvei	-	+
Rahnella aquatilis k 8	-	+
Rahnella genosp. 3 str. DSM 30078	+	+
Secondary symbiont type-U Acyrthosiphon pisum (rrs) clone 5B type-U	-	+
Yersinia aldovae str. A125	-	+
Desulfonauticus submarinus str. 6N	+	+
Desulfomicrobium baculatum str. DSM 1742	+	+
Desulfomicrobium baculatum str. X; VKM B-1378; DSM 4	+	+
Desulfovibrio sp. str. Ac5.2	+	+
Desulfovibrio hydrothermalis str. AM13	-	+
granular sludge clone R2b32	-	+
Desulfovibrio giganteus str. DSM 4370	+	+
termite gut homogenate clone Rs-N35 proteobacterium	+	+
termite gut homogenate clone Rs-M72 proteobacterium	+	+
Desulfovibrio desulfuricans	+	+
termite gut homogenate clone Rs-N31 proteobacterium	+	+
termite gut homogenate clone Rs-M89 proteobacterium	+	+
uranium mining waste pile clone JG37-AG-139 proteobacterium	+	+
forest soil clone S1204	+	+
heavy metal-contaminated soil clone a13134	+	+
Polyangium cellulosum str. 87-5	+	+
Polyangium cellulosum str. 9741	-	+
soil sample uranium mining waste pile near town Johanngeorgenstadt clone JG36-TzT-168 proteobacterium	+	+
marine tidal mat clone BTM36	+	-
Nannocystis exedens str. Na e571	+	+
sludge clone A9	+	+
hydrothermal sediment clone AF420357	+	+
Enhygromyxa salina str. SHK-1	+	-
uranium mining waste pile clone JG37-AG-15 proteobacterium	+	+
bacterioplankton clone ZA3704c	+	+
uranium mining waste pile clone JG34-KF-243 proteobacterium	+	+
bioreactor clone mle1-27	+	+
uranium mining waste pile clone JG34-KF-14 proteobacterium	+	+
Desulfuromonas sp. clone AKS68	+	+
Cytophaga sp. str. Dex80-43	+	+
DCP-dechlorinating consortium clone SHA-72	-	+
uranium mining waste pile clone JG37-AG-33 proteobacterium	+	+
marine sediment clone Bol11	+	+
Mono lake clone ML635J-58	+	+
Great Artesian Basin clone B83	+	+
Cytophaga sp. str. Dex80-64	+	+
deep marine sediment clone MB-A2-137	+	+
Antarctic sediment clone LH5_30	+	+
uranium mill tailings soil sample clone GuBH2-AD/TzT-67 proteobacterium	+	+
uranium mining waste pile clone JG37-AG-133 proteobacterium	+	+
deep marine sediment clone MB-B2-106	+	+

forested wetland clone RCP2-62	+	+
uranium mill tailings soil sample clone GuBH2-AG-114 proteobacterium	+	+
acid mine drainage clone AS6	+	+
hydrothermal sediment clone AF420341	+	+
uranium mill tailings soil sample clone Sh765B-TzT-29 proteobacterium	+	+
Great Artesian Basin clone G13	+	+
uranium mining waste pile clone JG37-AG-90 proteobacterium	+	+
bacterioplankton clone ZA3735c	+	+
Rocky Mountain alpine soil clone S1a-1H	+	+
uranium mining waste pile clone JG37-AG-128 proteobacterium	+	+
hydrothermal sediment clone AF420354	+	+
forested wetland clone FW140	+	-
forested wetland clone FW110	+	+
hydrothermal sediment clone AF420338	+	+
forest soil clone NOS7.157WL	+	+
granular sludge clone R1p32	+	+
granular sludge clone R3p4	+	+
Desulfacinum hydrothermale str. MT-96	+	+
DCP-dechlorinating consortium clone SHD-1	+	+
coal effluent wetland clone RCP185	+	+
forested wetland clone FW57	+	+
forested wetland clone FW13	+	+
TCE-contaminated site clone ccslm247	+	+
epibiontic clone C11-D3	+	+
marine sediment above hydrate ridge clone Hyd24-11 proteobacterium	+	+
inactive deep-sea hydrothermal vent chimneys clone IndB2-42	+	+
anoxic marine sediment clone LD1-PA38	+	+
Mono Lake at depth 23 m station 6 July 2000 clone ML623J-57 proteobacterium	+	+
Cytophaga sp. str. BHI60-57B	+	+
Psychrophilic sulfate-reducing isolate str. LSv23 bacterium	+	+
marine sediment above hydrate ridge clone Hyd01-n proteobacterium	+	+
Riftia pachyptila's tube clone R103-B13	+	+
gas hydrate clone Hyd89-51	+	+
uranium mining waste pile clone JG37-AG-30 proteobacterium	+	+
DCP-dechlorinating consortium clone SHA-51	+	+
benzoate-degrading consortium clone BA044	-	+
Syntrophus buswellii str. DSM 2612	-	+
Syntrophus gentianae str. HQgoe1	+	+
forested wetland clone FW117	+	+
acid mine drainage clone BA18	+	+
marine sediment above hydrate ridge clone Hyd89-61 proteobacterium	+	-
marine surface sediment clone SB2	+	+
temperate estuarine mud clone KM62	+	+
Desulfobacterium cetonicum str. DSM 7267 oil recovery water	+	-
sulfate-reducing habitat clone SLM-CP-116	+	+
sediment isolate str. EbS7	-	+
hydrothermal sediment clone AF420340	+	+
termite gut homogenate clone Rs-K70 proteobacterium	+	+

marine methane seep clone 1427	+	+
Antarctic sediment clone SB1_49	+	+
Guaymas Basin hydrothermal vent sediments clone B01R011	+	+
Guaymas Basin hydrothermal vent sediments clone B01R004	-	+
Antarctic sediment clone SB2_56	+	+
Flexispira rappini FH 9702248	+	+
Helicobacter heilmannii str. MM2	+	+
Helicobacter aurati str. MIT 97-5075c	+	+
Helicobacter cetorum str. MIT 99-5656	+	+
Helicobacter pylori str. 85D08	+	+
Helicobacter suncus str. Kaz-2	+	+
Helicobacter felis str. Dog-1	+	+
Helicobacter heilmannii str. C4S	+	+
Helicobacter pullorum str. NCTC 12826	+	+
Helicobacter rodentium str. MIT 96-1312	+	+
Helicobacter pylori str. ATCC 49396T	+	+
Helicobacter sp. blood isolate 964	+	+
Helicobacter rappini W.Tee-Bat	+	+
Helicobacter winghamensis str. NLEP 97-1611	+	+
Helicobacter rappini W.Tee-Yu	+	+
Helicobacter sp. 'liver 3' str. liver 3	+	+
hydrothermal vent clone PVB_10	-	+
termite gut homogenate clone Rs-P71 proteobacterium	+	+
Riftia pachyptila's tube clone R76-B51	+	+
hydrocarbon seep clone GCA014	-	+
strain isolate str. Dex60-82	-	+
hydrothermal sediment clone AF420359	-	+
hydrothermal vent polychaete mucous clone P. palm C 84	-	+
S17sBac16 complete clone	+	+
UASB reactor granular sludge clone PD-UASB-2 proteobacterium	-	+
hydrothermal vent 9 degrees North East Rise Pacific Ocean clone CH5_6_BAC_16SrRNA_9N_EPR	-	+
termite gut homogenate clone Rs-H40 proteobacterium	+	+
strain isolate str. BHI80-49	+	+
Arcobacter cryaerophilus	+	+
Sulfurospirillum deleyianum str. Spirillum 5175	-	+
Campylobacter sp. str. NO2B	-	+
temperate estuarine mud clone KM61	+	+
Campylobacter showae	+	-
Campylobacter helveticus	+	+
termite gut homogenate clone Rs-M59 proteobacterium	+	-
penguin droppings sediments clone KD8-87	+	+
magnetic coccus MP17	+	-
uranium mining waste pile near Johanngeorgenstadt soil clone JG37-AG-21	+	+
soil isolate Ellin301	+	+
lichen-dominated Antarctic cryptoendolithic community clone FBP483	+	-
termite gut homogenate clone Rs-J59 bacterium	-	+
ground water deep-well injection disposal site radioactive wastes Tomsk-7 clone S15A-MN100	+	+

termite gut homogenate clone Rs-J10 bacterium	-	+
Collinsella aerofaciens str. JCM7791	+	-
sponge clone TK39	+	-
bacterioplankton clone ZA3612c	+	+
forested wetland clone RCP1-37	+	+
forested wetland clone RCP1-77	-	+
forest soil clone DUNssu275 (-3A) (OTU#188)	+	+
	+	+
Mammoth cave clone CCM13a	+	+
forested wetland clone RCP2-105	+	+
bacterioplankton clone AEGEAN_247	+	+
marine sediment clone MB-A2-100	+	+
forested wetland clone RCP1-33	+	-
dilution (10e-7) brackish section Weser estuary isolate str. GP-5 GP-5	-	+
Sporichthya polymorpha str. IFO 12702	-	+
lichen-dominated Antarctic cryptoendolithic community clone FBP406	+	+
Frankia sp	-	+
Frankia sp. Sn5-8	+	+
Sturt arid-zone soil clone #0425-2M17	+	+
uranium mill tailings clone Gitt-KF-183	+	+
deep marine sediment clone MB-A2-108	+	+
uranium mining waste pile clone JG34-KF-418	+	+
lichen-dominated Antarctic cryptoendolithic community clone FBP417	-	+
soil clone #0319-7G21	+	+
Streptomyces galbus str. DSM40480	+	+
Streptomyces scabiei str. DNK-G01	+	+
Streptomyces cinnabarinus str. ISP 5467	+	+
Kitasatospora setae str. KM-6054	+	+
Streptacidiphilus carbonis str. JL 415; DSM 41754	-	+
Trichotomospora caesia str. IFO14562	+	+
Streptomyces subrutilus str. DSM 40445	+	+
soil clone 228-1	+	+
Kitasatospora cystarginea str. IFO14836T	+	+
soil clone 41-1	+	+
Streptomyces setonii str. ATCC25497	+	+
Streptomyces bikiniensis str. DSM40581	+	+
uranium mining waste pile soil sample clone JG30-KF-A23	+	+
earthworm burrow isolate B33D1	+	+
DCP-dechlorinating consortium clone SHA-34	+	+
marine sediment clone Bol7	+	+
Streptomyces sampsonii str. ATCC25495	+	+
Streptomyces coelicolor	+	+
Streptomyces coelicolor str. M145 ssp. A3(2)	+	+
hypersaline lake clone ML602J-44	+	+
Streptomonospora salina str. YIM90002	-	+
Nocardiopsis listeri str. DSM 40297T	-	+
Actinomadura pelletieri str. IMSNU 22169T	+	-
Actinomadura fulvescens str. DSM 43923T	+	+

Nonomuraea polychroma str. IFO 14345	+	+
Nonomuraea subsp. roseoviolacea str. SF 2303	-	+
Nonomuraea terrinata str. DSM 44505	-	+
Microbispora rosea subsp. aerata str. ATCC 27098	+	+
Rhodoglobus vestalii str. LV3	+	+
Leifsonia aquatica str. JCM1368	-	+
Firmicutes isolate str. d8	+	-
termite gut homogenate clone Rs-F20 bacterium	-	+
Microbacterium kitamiense CV88	+	-
Microbacterium lacticum	+	+
glacial ice isolate str. SB12K-2-1	+	+
Microbacterium sp. str. VKM Ac-2048	+	-
Cryocola antiquus str. VKM 103PF	+	+
Microbacterium resistens str. 2002-59119	+	+
Microbacterium sp. str. IFO16060	-	+
Arctic sea ice ARK10165	-	+
Arctic sea ice ARK10173	+	+
freshwater isolate str. MWH-Ta3	+	+
freshwater clone SV1-16	-	+
Rathayibacter rathayi str. DSM 7485	+	+
Georgenia muralis str. 1A-C	+	+
penguin droppings sediments clone KD3-138	+	+
Cellulomonadaceae str. WB9	+	+
Cellulomonadaceae str. W6	+	+
Cellulomonadaceae str. WB13	-	+
Cellulomonas gelida str. DSM 20111T	+	+
Cellulosimicrobium cellulans str. NCIMB 11025	+	+
Jonesia quinghaiensis str. DSM 15701	+	+
Promicromonospora sukumoe str. DSM 44121	+	+
Beutenbergia cavernosa str. DSM 12333	+	+
Actinobacteria str. VeCb6	+	+
termite gut homogenate clone Rs-M95 bacterium	+	+
Arthrobacter psychrolactophilus	+	+
Arthrobacter oxydans str. DSM 20119	+	+
Arthrobacter globiformis	+	+
Arthrobacter sp str. AC-51	+	+
Varibaculum cambriense str. CCUG 44998	+	+
Yania halotolerans str. YIM 70085	+	+
TCE-contaminated site clone ccspost2208	+	+
glacial ice isolate str. CanDirty1	+	+
Arthrobacter agilis str. DSM 20550	+	+
termite gut homogenate clone Rs-N91 bacterium	+	+
termite gut homogenate clone Rs-M66 bacterium	-	+
Arthrobacter ureafaciens str. DSM 20126	+	+
Arthrobacter nicotianae str. SB42	+	+
Micrococcus luteus str. HN2-11	+	+
Kocuria roseus	+	+
Kocuria rhizophila str. KL-057	-	+

Brevibacterium iodinum str. DSM 2062T	+	+
Brachybacterium sacelli str. LMG 20338	-	+
Brachybacterium conglomeratum str. NCIB 9859	-	+
Brachybacterium nesterenkovii str. DSM 9573	+	+
Actinomyces naeslundii	+	+
Arcanobacterium haemolyticum str. CIP 103370	-	+
Bifidobacterium psychraerophilum str. T16	+	+
Bifidobacterium pseudocatenulatum str. JCM1200	-	+
Bifidobacterium adolescentis str. E-981074T	-	+
Bifidobacterium thermacidophilum porcinum subsp. suis str. P3-14 subsp.	-	+
Bifidobacteriaceae genomosp. C1	-	+
Bifidobacterium breve str. KB 92	-	+
Kineosporia aurantiaca str. JCM3230	+	+
lichen-dominated Antarctic cryptoendolithic community clone FBP402	+	+
endemic to Mojave Desert isolate str. AS3138 AS3138	-	+
Kineococcus aurantiacus str. IFO 15268	+	+
Aeromicrobium erythreum str. NRRL B-3381	-	+
Aeromicrobium marinum str. T2	-	+
Nocardioides sp. str. V4.BO.15 = MM_2364	+	+
Actinoplanes utahensis str. IMSNU 20044T	+	+
related to BDA1-5 (Marine Gram-positive) Actinomycetes clone OCS155 OCS155	+	+
Actinoplanes roseosporangius str. IMSNU 22133	+	+
Actinoplanes capillaceus str. K95-5561	+	+
Actinoplanes garbadinensis str. IMSNU 20040	+	+
Actinoplanes derwentensis str. IFO 14935T	+	+
Actinoplanes tuftoflagellus str. IMSNU 22135	+	+
Actinoplanes utahensis str. ATCC 31044	+	+
Actinoplanes regularis str. IFO 12514T	+	+
Actinoplanes yunnanensis str. IFO 14459T	+	+
Couchioplanes subsp. caeruleus str. IFO13939	+	+
Couchioplanes subsp. caeruleus str. IFO13939	+	+
acid mine drainage clone ASL8	+	+
Actinoplanes durhamensis str. IMSNU 22124T	+	+
Micromonospora marina str. JSM3-1	+	+
Catellatospora subsp. citrea str. IMSNU 22008T subsp.	-	+
Amycolatopsis mediterranei str. NRRL B-3240	+	+
Amycolatopsis tolypomycina str. DSM 44544	+	-
Amycolatopsis mediterranei str. IMSNU 20056T	+	-
Amycolatopsis sulphurea str. IMSNU 20060T	+	+
Amycolatopsis vancoresmycina str. DSM 44592	+	-
Saccharomonospora azurea str. M.Goodfel K161=NA128 (type st	+	+
Mycobacterium cf. xenopi 'Hymi_Wue Tb_939/99' str. Hymi_Wue Tb_939/99	+	+
Mycobacterium palustre str. E846	+	+
Mycobacterium aichiense str. JS618	+	+
Mycobacterium sp. 3	+	+
Mycobacterium ratisbonense str. SD4	-	+
Mycobacterium holsaticum str. 1406	+	+
Mycobacterium pyrenivorans str. DSM 44605	+	+

USA: Colorado Fort collins Horsetooth Reservoir clone HTDD3	+	+
Mycobacterium chelonae str. CIP 104535T	+	+
Mycobacterium cf. triplex 'isolate 23' 23	+	+
Mycobacterium tuberculosis str. NCTC 7416 H37Rv	+	+
Mycobacterium sp. str. 1B(CD)	+	+
Mycobacterium terrae str. ATCC 15755	+	+
Mycobacterium rhodesiae str. JS60	+	+
Mycobacterium marinum	+	+
Mycobacterium neoaurum str. ATCC 25795	+	+
Mycobacterium brisbanense str. W6743; ATCC 49938	-	+
Mycobacterium chlorophenolicum str. PCP-I	+	+
Gordona terrae	+	+
Gordonia alkanivorans	+	+
Gordonia amarae str. DSM43392	-	+
Gordonia polyisoprenivorans str. Y2K	+	+
Dietzia maris	-	+
Corynebacterium xerosis str. DSM 20743	+	+
Corynebacterium tuscaniae str. ISS-5309	+	+
Corynebacterium jeikeium str. ATCC 43734	+	+
Corynebacterium mucifaciens National Microbiology Laboratory Special identifier 01-0118	+	+
Corynebacterium simulans National Microbiology Laboratory Special identifier 00-0186	+	+
Corynebacterium spheniscorum str. CCUG 45512	+	+
polluted aquifer clone BVC83	+	+
Rhodococcus ruber str. DSM43338	+	+
forested wetland clone RCP2-103	+	+
Rhodococcus opacus str. B-4	+	+
Rhodococcus corynebacterioides str. DSM 20151	-	+
Rhodococcus species	-	+
Dietzia sp. str. E9_2	-	+
Nocardia otitidiscaviarum str. S639	+	+
Nocardia caishijiensis str. F829	-	+
Nocardia sp. str. 99-08-244A	-	+
Nocardia veterana str. DSM 44445	-	+
Nocardia yamanashiensis str. IFM 0265	+	+
Nocardia cyriacigeorgica str. D1627T	-	+
Nocardia pseudovaccinii str. DSM 43406	+	+
Nocardia transvalensis str. DSM 43405	+	+
Nocardia otitidiscaviarum str. DSM43242	+	+
Nocardia uniformis str. DSM 43136	+	+
Desulfotomaculum thermobenzoicum str. DSM 6193	+	+
UASB granular sludge clone JP	+	+
G+C Gram-positive clone YNPRH70A	+	+
Desulfotomaculum thermoacetoxidans str. DSM 5813	+	+
Natronoanaerobium aggerbacterium G-M16NWC-4	-	+
Desulfotomaculum solfataricum str. V21	+	+
UASB granular sludge clone UT-2	-	+
saltmarsh clone LCP-89	+	+

granular sludge clone R4b14	+	+
trichloroethene-contaminated site clone FTLM142 bacterium	+	+
uranium mining waste pile soil clone JG30-KF-C12	+	+
Guaymas Basin hydrothermal vent sediments clone B03R012	+	-
deep marine sediment clone MB-C2-106	-	+
Mono Lake at depth 23m station 6 July 2000 clone ML623J-19	+	+
Guaymas Basin hydrothermal vent sediments clone B01R005	+	-
deep marine sediment clone MB-B2-103	+	-
anoxic marine sediment clone LD1-PA39	+	+
anaerobic sludge isolate str. JE	+	+
Thermaerobacter marianensis	+	+
Thermaerobacter nagasakiensis str. JCM 11223	+	+
TCE-contaminated site clone FTL22	+	+
sponge symbiont clone TK19	+	+
uranium mill tailings soil clone Sh765B-TzT/AG-5	+	+
uranium mill tailings soil sample clone Sh765B-TzT-20 bacterium	+	+
deep marine sediment clone MB-B2-113	+	+
Dehalococcoides ethenogenes str. strain 195	+	+
deep marine sediment clone MB-C2-127	+	+
deep marine sediment clone MB-A2-110	+	+
deep marine sediment clone MB-A2-103	+	-
uranium mill tailings soil sample clone Sh765B-TzT-6 bacterium	+	+
forested wetland clone FW60	+	+
sponge clone TK10	+	+
penguin droppings sediments clone KD4-96	+	-
forest soil clone C083	+	+
trichloroethene-contaminated site clone FTL276 bacterium	+	+
forest soil clone S085	+	+
hydrothermal vent clone VC2.1Bac23	+	-
Thermovibrio ammoniificans str. HB-1	+	+
Selenomonas ruminantium str.JCM6582	+	+
Anaerovibrio lipolyticus str. ATCC 33276	-	+
Selenomonas ruminantium str.S20	+	+
Centipeda periodontii str. HB-2	+	+
pig feces clone	+	+
Dialister invisus str. E7_25	+	+
Great Artesian Basin clone G07	+	+
DCP-dechlorinating consortium clone SHA-109	+	+
chlorobenzene-degrading consortium clone IIA-26	+	+
thermal soil clone YNPFFP9	+	+
anoxic bulk soil flooded rice microcosm clone BSV43 clone	+	+
termite gut homogenate clone Rs-J36 bacterium	-	+
MCB-contaminated groundwater-treating reactor clone RB9C2	-	+
termite gut homogenate clone Rs-P50 bacterium	+	+
Desulfosporosinus orientis str. DSMZ 7493	+	-
deep marine sediment clone MB-C2-152	+	+
termite gut homogenate clone Rs-A28 bacterium	+	+
drinking water system simulator clone HOClCi9	-	+

benzene-contaminated groundwater clone ZZ12C8	+	+
forested wetland clone RCP2-71	+	+
UASB granular sludge clone UT-1	-	+
termite gut homogenate clone Rs-B88 bacterium	+	-
swine intestine clone p-3075-SwA5	+	+
swine intestine clone p-2876-6C5	+	+
rumen clone 6C3d-11	+	+
termite gut homogenate clone Rs-F27 bacterium	+	+
termite gut homogenate clone Rs-G40 bacterium	+	+
termite gut homogenate clone Rs-D48 bacterium	+	+
Clostridium nexile	+	+
anaerobic digester clone AA02	-	+
human stool clone B065	+	+
termite gut clone Rs-L15	+	+
human colonic clone HuCA20	+	+
oxidoreducens str. G2-2	-	+
swine intestine clone p-1594-c5	+	+
Lachnospira pectinoschiza	+	+
ruminantium str. GA195	+	-
TCE-dechlorinating microbial community clone 4C	-	+
termite gut homogenate clone Rs-G77 bacterium	+	+
termite gut homogenate clone Rs-B14 bacterium	+	+
termite gut homogenate clone Rs-N53	+	+
termite gut homogenate clone Rs-K41 bacterium	+	+
termite gut homogenate clone Rs-F76 bacterium	+	+
termite gut homogenate clone Rs-N71 bacterium	+	+
DCP-dechlorinating consortium clone SHA-58	+	+
termite gut homogenate clone BCf9-13	+	+
oral periodontitis clone FX028	+	+
termite gut homogenate clone Rs-N27 bacterium	+	+
termite gut homogenate clone Rs-E61 bacterium	+	+
termite gut homogenate clone Rs-N82 bacterium	+	+
termite gut homogenate clone Rs-F43 bacterium	+	+
Evry municipal wastewater treatment plant clone 012C11_B_SD_P15	+	+
termite gut homogenate clone Rs-Q64 bacterium	+	+
chlorobenzene-degrading consortium clone IA-19	+	+
oral clone P2PB_46 P3	-	+
oral periodontitis clone FX033	-	+
Clostridium caminithermale str. DVird3	+	+
coal effluent wetland clone RCP216	+	+
Great Artesian Basin clone R82	-	+
human subgingival plaque clone BB142	+	-
Tepidibacter thalassicus str. SC 562	+	+
Clostridium paradoxum str. DSM 7308T	-	+
Clostridium paradoxum str. DSM 7308T	-	+
midgut homogenate Pachnoda ephippiata larva clone PeM47	+	+
Isolation and identification hyper-ammonia producing swine storage pits manure	+	+
termite gut homogenate clone Rs-H81 bacterium	+	+

Sedimentibacter sp. str. BRS2	+	-
oral periodontitis clone EX153	+	+
Peptostreptococcaceae bacterium 19gly3	-	+
TCE-dechlorinating microbial community clone 1G	+	+
Finegoldia magna str. ATCC 29328	+	+
Peptostreptococcus sp. str. E3_32	+	+
Finegoldia magna	+	+
Peptostreptococcus sp. oral clone P4PA_156 P4 oral	+	+
Peptoniphilus lacrimalis str. CCUG 31350	-	+
Anaerococcus vaginalis str. CCUG 31349	+	+
geothermal site isolate str. G1	+	+
Bacillus schlegelii str. ATCC 43741T	+	+
Paenibacillus nematophilus str. NEM1b	+	+
Paenibacillus turicensis str. MOL722	+	+
Paenibacillus borealis KK20	+	+
Paenibacillus sp. str. MB 2039	+	+
Paenibacillus thiaminolyticus str. DSM 7262	-	+
Bacillus sp. clone ML1228J-1	+	+
Brevibacillus borstelensis str. LMG 15536	+	+
Brevibacillus sp. MN 47.2a	+	-
Laceyella sacchari str. KCTC 9789 ()	-	+
Bacillus sp. clone ML615J-19	+	+
Bacillus algicola str. KMM 3737	+	+
uranium mill tailings clone Gitt-KF-76	+	+
Bacillus clausii str. GMBAE 42	+	+
Bacillus sp. str. 2216.25.2	+	+
Bacillus sp. str. SAFN-006	+	+
Bacillus baekryungensis str. SW-93	+	+
Lake Elmenteita isolate WE4	-	+
Bacillus vulcani str. 3S-1	+	+
Geobacillus thermocatenulatus str. DSM 730	+	+
Bacillus thermoleovorans	+	+
Thermoactinomyces sp. str. 700375	+	+
Geobacillus jurassicus str. DS1	+	+
Geobacillus caldoxylosilyticus str. BGSC W98A1	-	-
Geobacillus thermoleovorans str. B23	+	+
Geobacillus stearothermophilus	+	+
Geobacillus stearothermophilus str. 46	+	+
Geobacillus stearothermophilus str. T10	+	+
Geobacillus thermodenitrificans str. DSM 466	+	+
Bacillus caldotenax str. DSM 406	+	+
Geobacillus sp. str. YMTC1049	+	+
Bacillus acidogenesis str. 105-2	+	+
Halobacillus yeomjeoni str. MSS-402	+	+
Salibacillus sp. str. YIM-kkny16	+	+
Bacillus niacini str. IFO15566	+	+
Bacillus siralis str. 171544	+	+
Bacillus senegalensis str. RS8; CIP 106 669	+	+

anoxic bulk soil flooded rice microcosm clone BSV45 clone	+	-
anoxic bulk soil flooded rice microcosm clone BSV46 clone	+	+
Bacillus firmus str. NCIMB 9366	+	+
Bacillus litoralis str. SW-211	+	-
Bacillus simplex str. DSM 1321T	+	-
Bacillus megaterium str. QM B1551	+	+
Bacillus sp. str. KL-152	+	-
Bacillus pumilus str. S9	-	+
Pseudobacillus carolinae	+	+
Bacillus licheniformis str. SAFN-031	+	+
Bacillus subtilis str. IAM 12118T	+	+
Bacillus sp. str. TGS750	+	+
Bacillus licheniformis str. SK-1	+	+
Bacillus mojavensis str. M-1	+	+
Bacillus sonorensis str. NRRL B-23155	+	+
Bacillus licheniformis str. Mo1	+	+
Bacillus licheniformis str. KL-068	+	+
Bacillus licheniformis str. DSM 13	+	+
Bacillus subtilis subsp. Marburg str. 168	+	+
Bacillus subtilis	+	+
Staphylococcus auricularis str. MAFF911484 ATCC33753T	-	-
Staphylococcus sp str. AG-30	+	+
Bacillus luciferensis str. LMG 18422	+	+
Bacillus sphaericus	+	+
Caryophanon latum str. DSM 14151	+	+
Bacillus silvestris str. SAFN-010	-	+
garbage compost isolate str. M32	-	+
Sporosarcina macmurdoensis str. CMS 21w	+	+
Planococcus maritimus str. TF-9	+	+
Bacillus psychrodurans str. DSM 11713 68E3	+	+
compost clone 4-28	+	+
feedlot manure clone B87	+	+
Lactobacillus kitasatonis str. KM9212	-	+
Lactobacillus suntoryeus str. LH	-	+
Lactobacillus reuteri str. DSM 20016 T	-	+
Lactobacillus frumenti str. TMW 1.666	+	+
Lactobacillus pontis str. LTH 2587	+	+
Pediococcus inopinatus str. DSM 20285	-	+
Pediococcus pentosaceus	-	+
Lactobacillus letivazi str. JCL3994	-	+
Lactobacillus subsp. aviarius	+	+
Lactobacillus perolens str. L532	+	+
cf. Alkalibacterium sp. isolate str. F1	+	+
Carnobacterium alterfunditum	-	+
Enterococcus mundtii str. LMG 10748	+	+
Enterococcus saccharolyticus str. LMG 11427	+	+
Tetragenococcus muriaticus	+	+
Enterococcus solitarius str. DSM 5634	+	+

Enterococcus cecorum str. ATCC43198	+	+
Enterococcus dispar str. LMG 13521	+	+
Lactococcus Il1403 subsp. lactis str. IL1403	+	+
Streptococcus equi subsp. zooepidemicus str. Tokyo1291 subsp.	+	+
Streptococcus thermophilus str. DSM 20617	+	+
Streptococcus constellatus str. ATCC27823	+	+
Streptococcus suis str. 8074	+	+
Streptococcus cristatus str. ATCC 51100	+	+
Streptococcus mitis str. Sm91	-	+
Streptococcus gordonii str. ATCC 10558	+	+
Weeping tea tree witches'-broom phytoplasma tree	+	-
Ash witches'-broom phytoplasma str. AshWB	-	+
Chinaberry yellows phytoplasma str. CbY1	-	+
Australia isolate str. BVGY	-	-
Eubacterium cylindroides	+	+
Streptococcus pleomorphus	+	+
TCE-contaminated site clone ccslm238	+	+
phototrophic sludge clone PSB-M-3	+	+
Mycoplasma gypsbengalensis str. Gb-V33	+	+
Mycoplasma zalophus str. 4296C	-	+
MCB-contaminated groundwater-treating reactor clone RA9C1	+	+
Clostridiales oral clone P4PB_122 P3	+	+
forested wetland clone FW105	+	-
granular sludge clone R1p16	+	+
termite gut clone Rs-L02	+	+
termite gut clone Rs-060	+	+
termite gut clone Rs-056	+	+
oral endodontic infection clone MCE3_9	+	+
Mono Lake at depth 35m station 6 July 2000 clone ML635J-65 G+C	+	+
termite gut homogenate clone Rs-J39 bacterium	+	+
termite gut homogenate clone Rs-N85 bacterium	+	+
termite gut homogenate clone Rs-H83 bacterium	+	+
Mono Lake at depth 35m station 6 July 2000 clone ML635J-14 G+C	-	+
Clostridium papyrosolvens str. DSM 2782	+	+
Clostridium sp. str. JC3	+	+
Mono Lake at depth 35m station 6 July 2000 clone ML635J-21 G+C	+	+
termite gut clone Rs-068	+	+
termite gut homogenate clone Rs-K92 bacterium	-	+
termite gut homogenate clone Rs-A15 bacterium	+	+
ckncm322-B3-7 clone	+	+
termite gut homogenate clone Rs-M23 bacterium	+	+
termite gut clone Rs-061	+	+
termite gut clone Rs-116	+	+
termite gut homogenate clone Rs-G04 bacterium	+	+
termite gut homogenate clone Rs-M86 bacterium	+	-
termite gut clone Rs-114	+	+
termite gut homogenate clone Rs-M34 bacterium	+	+
termite gut homogenate clone Rs-M14 bacterium	+	+

granular sludge clone UASB_brew_B86	+	+
termite gut homogenate clone Rs-Q01 bacterium	+	+
human mouth clone P4PA_66	+	+
termite gut homogenate clone Rs-N94 bacterium	+	+
termite gut homogenate clone Rs-C76 bacterium	+	-
Oscillospira guilliermondii	-	+
granular sludge clone UASB_brew_B84	+	+
termite gut homogenate clone Rs-N86 bacterium	+	+
Lachnospiraceae bacterium 19gly4	-	+
termite gut homogenate clone Rs-C69 bacterium	+	+
termite gut homogenate clone Rs-N73 bacterium	+	+
ckncm301-B3-28 clone	+	+
termite gut homogenate clone Rs-K32 bacterium	+	-
termite gut homogenate clone Rs-H18 bacterium	+	-
termite gut homogenate clone Rs-K11 bacterium	+	+
termite gut clone Rs-109	+	+
termite gut clone Rs-058	+	+
termite gut homogenate clone Rs-N02 bacterium	+	+
termite gut homogenate clone Rs-N21 bacterium	+	+
termite gut homogenate clone Rs-Q53 bacterium	+	+
ckncm314-B7-17 clone	+	+
granular sludge clone UASB_brew_B25	+	+
termite gut homogenate clone Rs-B34 bacterium	+	+
termite gut clone Rs-093	+	+
termite gut homogenate clone Rs-N06 bacterium	+	+
ckncm297-B1-1 clone	+	+
termite gut homogenate clone Rs-M18 bacterium	+	+
termite gut homogenate clone Rs-Q69 bacterium	-	+
swine intestine clone p-2657-65A5	-	+
human colonic clone HuCB5	+	+
Faecalibacterium prausnitzii str. ATCC 27766	+	+
rumen clone 3C0d-3	+	+
termite gut homogenate clone Rs-A13 bacterium	+	+
UASB reactor granular sludge clone PD-UASB-4 bacterium	+	+
termite gut homogenate clone Rs-K21 bacterium	+	+
TCE-contaminated site clone ccslm210	+	+
Clostridium tyrobutyricum str. NIZO 51	+	+
Clostridium tyrobutyricum	+	+
Clostridiaceae str. A4d	+	+
rumen clone F23-C12	+	+
termite gut homogenate clone Rs-Q18 bacterium	+	+
Clostridium subterminale str. NCIMB 10746	-	+
Clostridium acetobutylicum str. ATCC 824 (T)	+	+
Clostridium acetobutylicum str. ATCC 824	-	+
Clostridium butyricum str. ATCC43755	+	+

An OTU was considered present in the sample when 90% or more of its assigned probe pairs for its corresponding probe set were positive (positive fraction of >0.90).